

การสังเคราะห์ตัวเร่งปฏิกิริยาออกไซด์ผสมของนิกเกิล/แมกนีเซียม/เซอร์โคเนียมด้วยวิธีตกตะกอนร่วม



นายชาญศักดิ์ สุกแก้ว

สถาบันวิทยบริการ

วิทยานิพนธ์นี้เป็นส่วนหนึ่งของการศึกษาตามหลักสูตรปริญญาวิทยาศาสตรมหาบัณฑิต

สาขาวิชาปิโตรเคมีและวิทยาศาสตร์พอลิเมอร์

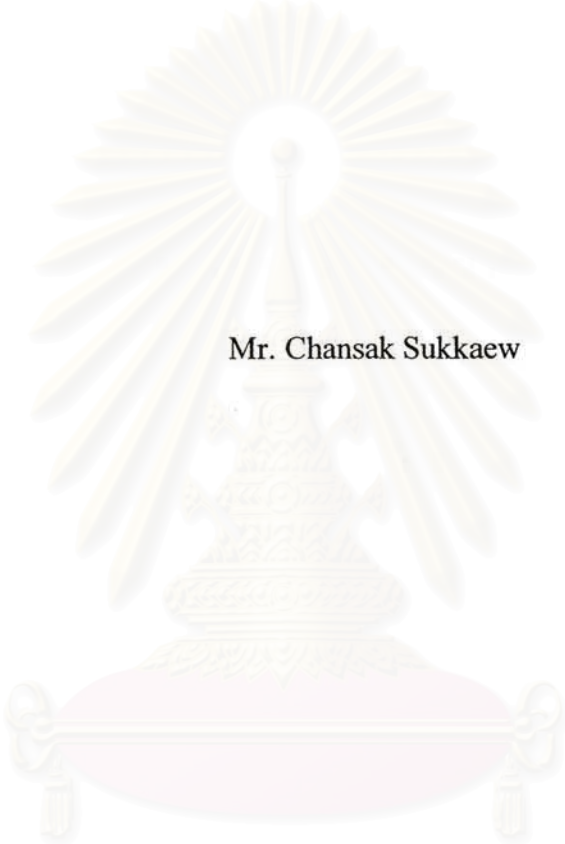
คณะวิทยาศาสตร์ จุฬาลงกรณ์มหาวิทยาลัย

ปีการศึกษา 2548

ISBN : 974-53-2748-4

ลิขสิทธิ์จุฬาลงกรณ์มหาวิทยาลัย

**SYNTHESIS OF NICKEL/MAGNESIUM/ZIRCONIUM MIXED OXIDE
CATALYSTS BY CO-PRECIPITATION METHOD**



Mr. Chansak Sukkaew

สถาบันวิทยบริการ
จุฬาลงกรณ์มหาวิทยาลัย

A Thesis Submitted in Partial Fulfillment of the Requirements
for the Degree of Master of Science Program in Petrochemistry and Polymer Science

Faculty of Science

Chulalongkorn University

Academic Year 2005

ISBN : 974-53-2748-4

Thesis Title SYNTHESIS OF NICKEL/MAGNESIUM/ZIRCONIUM MIXED
OXIDE CATALYSTS BY CO-PRECIPITATION METHOD

By Mr. Chansak Sukkaew

Field of Study Petrochemistry and Polymer Science

Thesis Advisor Associate Professor Wimonrat Trakarnpruk, Ph.D.

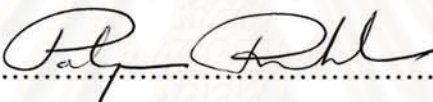
Accepted by the Faculty of Science, Chulalongkorn University in Partial
Fulfillment of the Requirements for the Master's Degree



.....Dean of the Faculty of Science

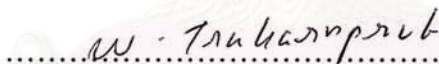
(Professor Piamsak Menasveta, Ph.D.)

THESIS COMMITTEE



.....Chairman

(Professor Pattarapan Prasassarakich, Ph.D.)



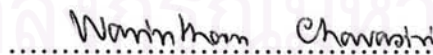
..... Thesis Advisor

(Associate Professor Wimonrat Trakarnpruk, Ph.D.)



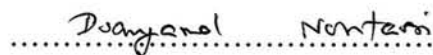
.....Member

(Associate Professor Supawan Tantayanon, Ph.D.)



.....Member

(Assistant Professor Warinthorn Chavasiri, Ph.D.)



.....Member

(Duangamol Nuntasri, Ph.D.)

ชาญศักดิ์ สุขแก้ว : การสังเคราะห์ตัวเร่งปฏิกิริยาออกไซด์ผสมของนิกเกิล/แมกนีเซียม/เซอร์โคเนียมด้วยวิธีตกตะกอนร่วม (SYNTHESIS OF NICKEL/MAGNESIUM/ZIRCONIUM MIXED OXIDE CATALYSTS BY CO-PRECIPIATION METHOD)
 อ.ที่ปรึกษา: รศ. ดร. วิมลรัตน์ ตระการพุกฤษ, 71 หน้า ISBN: 974-53-2748-4

ได้เตรียมตัวเร่งปฏิกิริยาออกไซด์ผสมของนิกเกิล/แมกนีเซียม/เซอร์โคเนียม จากวิธีการเตรียมที่ต่างกัน 4 วิธี ได้แก่ การตกตะกอนร่วม co-precipitation (CP), ฟรีเคอเซอร์ซิติกแอซิด citric acid precursor technique (CT), ฟรีเคอเซอร์ซิติกแอซิดที่มีการดัดแปร modified citric acid precursor technique (MCT), ฟรีเคอเซอร์ซิติกแอซิด/เอทิลีนไกลคอลที่มีการดัดแปร modified citric acid/ethylene glycol precursor technique (MCTE) ได้พิสูจน์เอกลักษณ์ของตัวเร่งปฏิกิริยาด้วยเทคนิคการเลี้ยวเบนรังสีเอกซ์ (XRD), กล้องอิเล็กตรอนแบบส่องผ่าน (TEM), กล้องอิเล็กตรอนแบบส่องกราด (SEM), การวิเคราะห์รังสีเอกซ์แบบกระจายพลังงาน (EDX), ฟูเรียทรานสฟอร์มอินฟราเรดสเปกโทรสโคปี (FTIR), การวิเคราะห์เทอร์โมเกรวิเมตริก (TGA) และ Brunauer-Emmet-Teller (BET) ได้ศึกษาตัวแปรที่มีผลต่อลักษณะและสมบัติของออกไซด์ผสมของนิกเกิล/แมกนีเซียม/เซอร์โคเนียม ได้แก่ สัดส่วนโดยโมลของแมกนีเซียม/เซอร์โคเนียม ปริมาณโลหะนิกเกิล อุณหภูมิในการเผา เวลาในการเผา สารเติมแต่งดีบุก (Sn) จากผล XRD พบว่า เมื่อใช้สัดส่วนโดยโมลของแมกนีเซียม/เซอร์โคเนียม เท่ากับ 4 และปริมาณนิกเกิล 15% โดยน้ำหนัก ออกไซด์อยู่ในรูปเฟส cubic Mg-ZrO₂ การเตรียมออกไซด์ผสมด้วยวิธี CP ใช้อุณหภูมิในการเผาที่ต่ำกว่าวิธีอื่น (600°C) ให้ออกไซด์ผสมที่มีพื้นที่ผิว 136 ตารางเมตร/กรัม และขนาดรูพรุนที่เล็ก ส่วนการเตรียมด้วยวิธี CT ซึ่งเป็นวิธีที่มีการเผาเพียงครั้งเดียว ใช้อุณหภูมิในการเผาที่สูง (800°C) ให้ออกไซด์ผสมที่มีพื้นที่ผิวน้อยที่สุด และมีขนาดรูพรุนที่เล็ก วิธี MCT ซึ่งมีการเผา 2 ครั้ง ให้ออกไซด์ที่มีพื้นที่ผิวสูง (145 ตารางเมตร/กรัม) และขนาดรูพรุนที่ใหญ่ สำหรับวิธี MCTE ให้พื้นที่ผิวที่สูง (144 ตารางเมตร/กรัม) ลักษณะพื้นที่ผิวที่ได้จากเทคนิค SEM แสดงให้เห็นอนุภาคโลหะรูปร่างกลม มีขนาดอนุภาคในระดับนาโนเมตร

สาขาวิชา ปิโตรเคมีและวิทยาศาสตร์พอลิเมอร์ ลายมือชื่อนิสิต ชาญศักดิ์ สุขแก้ว
 ปีการศึกษา 2548 ลายมือชื่ออาจารย์ที่ปรึกษา วิมลรัตน์ ตระการพุกฤษ

4772272023: MAJOR PETROCHEMISTRY AND POLYMER SCIENCE

KEY WORD: MIXED OXIDE / CO-PRECIPIATION METHOD

**CHANSAK SUKKAEW: SYNTHESIS OF NICKEL/MAGNESIUM/
ZIRCONIUM MIXED OXIDE CATALYSTS BY CO-
PRECIPITATION METHOD. THESIS ADVISOR: ASSOC. PROF.
WIMONRAT TRAKARNPRUK, Ph.D., 71 pp ISBN: 974-53-2748-4**

Mixed metal oxide catalysts of Ni/Mg/Zr were prepared by four different methods: co-precipitation (CP), citrate precursor technique (CT), modified citric acid precursor technique (MCT), modified citric acid/ethylene glycol precursor technique (MCTE). The mixed metal oxides were characterized by several techniques: X-ray Diffraction (XRD), Transmission Electron Microscopy (TEM), Scanning Electron Microscopy (SEM), Energy Dispersive X-ray Analysis (EDX), Fourier Transform Infrared spectroscopy (FTIR), Thermogravimetric Analysis (TGA) and Brunauer-Emmet-Teller (BET). Parameters influencing the characteristics and properties of the mixed metal oxides were studied, such as Mg/Zr molar ratio, Ni content, calcination temperature, calcination time and additive (Sn). It was found from the XRD results that when using Mg/Zr molar ratio at 4 and 15% wt Ni, the mixed metal oxide exists as cubic Mg-ZrO₂ phase. In the CP method, calcination was performed at lower temperature (600°C), it yielded oxides with surface area of 136 m²/g and small pore size. In the CT method in which one calcination was performed at high temperature (800°C), the oxides had very low surface area and pore size. By MCT method in which two calcinations were performed, it yielded oxides with high surface area (145 m²/g) and large pore size. The MCTE method also yielded oxides with high surface area (144 m²/g). The morphology of the oxides observed by SEM showed that the oxides had spherical shape with nanosize.

Field of Study Petrochemistry and Polymer Science Student's signature Chansak Sukkaew

Academic year 2005 Advisor's signature Wimonrat Trakarnpruk

ACKNOWLEDGEMENTS

The author wishes to express his greatest gratitude to his advisor, Associate Professor Dr. Wimonrat Trakarnpruk, for her advice, assistance and generous encouragement throughout the course of this research. In addition, he wishes to express deep appreciation to Professor Dr. Pattarapan Prasassarakich, Associate Professor Dr. Supawan Tantayanon, Assistant Professor Dr. Warinthorn Chavasiri and Dr. Duangamol Nuntasri for serving as the chairman and member of thesis committee, respectively, for their valuable suggestion and comments.

Appreciation is also extended to the Program of Petrochemistry and Polymer Science and the Department of Chemistry, Faculty of Science, Chulalongkorn University for provision of experimental facilities. He also acknowledges the Graduate School for granting financial support for this study.

Finally he is very appreciated to his family and good friends for their assistance and encouragement.



สถาบันวิทยบริการ
จุฬาลงกรณ์มหาวิทยาลัย

CONTENTS

	Page
ABSTRACT IN THAI.....	iv
ABSTRACT IN ENGLISH.....	v
ACKNOWLEDGEMENTS.....	vi
CONTENTS.....	vii
LIST OF FIGURES.....	x
LIST OF TABLES.....	xii
LIST OF SCHEMES.....	xiii
LIST OF ABBREVIATION.....	xiv
CHAPTER I INTRODUCTION.....	1
1.1 Methane reforming.....	1
1.2 Statement of problem.....	1
1.3 The objective of the thesis.....	2
1.4 The scope of the thesis.....	2
CHAPTER II THEORY AND LITERATURE REVIEWS.....	4
2.1 Theory.....	4
2.1.1 Catalytic reforming of methane.....	4
2.1.2 X-ray diffraction (XRD).....	5
2.1.3 Brunauer-Emmett-Teller method (BET).....	6
2.1.4 Barrett–Joyner–Halenda method (BJH).....	8
2.1.5 Energy dispersive X-ray analysis (EDX).....	9
2.1.6 Scanning electron microscopy (SEM).....	10
2.1.7 Fourier transform infrared spectroscopy (FTIR).....	11
2.1.8 Transmission electron microscopy (TEM)	11
2.2 Literature reviews.....	12
CHAPTER III EXPERIMENTAL.....	16
3.1 Chemicals.....	16
3.2 Equipment and apparatus.....	17

	Page
3.3	Characterization methods..... 18
3.3.1	Fourier-transform infrared spectroscopy (FT-IR).....18
3.3.2	X-ray powder diffraction (XRD).....18
3.3.3	Nitrogen adsorption (BET).....18
3.3.4	Transmission electron microscopy (TEM).....18
3.3.5	Scanning electron microscopy (SEM).....19
3.3.6	Thermogravimetric analyzer (TGA).....19
3.4	Synthesis of mixed oxides of Ni/Mg/Zr
A.	Coprecipitation method (CP).....19
B.	Citric acid precursor method (CT).....20
C.	Modified citric acid precursor method (MCT).....21
D.	Modified citric acid/ethylene glycol precursor method (MCTE).....22
E.	Sn doping.....23
CHAPTER IV RESULT AND DISCUSSION.....25	
4.1	Single metal oxides and binary oxide of Mg/Zr.....25
4.2.	Mixed oxides catalysts prepared by co-precipitation (CP).....26
4.2.1	Effect of calcination temperature.....26
4.2.2	Effect of calcination time.....28
4.2.3	Effect of Mg/Zr molar ratio30
4.2.4	Effect of % Ni.....33
4.3	Citrate precursor technique (CT).....35
4.3.1	Effect of calcination temperature.....35
4.3.2	Effect of calcination time.....36
4.3.3	Effect of Mg/Zr molar ratio38
4.3.4	Effect of citric acid content.....40
4.4	Modified citric acid precursor technique (MCT).....42
4.5	Modified citric acid/ethylene glycol precursor technique (MCTE).....46

	Page
4.6 Characterization	48
4.6.1 Fourier-transform infrared spectroscopy (FT-IR).....	48
4.6.2 Energy Dispersive X-ray Analysis (EDX).....	49
4.6.3 Scanning electron microscopy (SEM).....	50
4.6.4 Transmission electron microscopy (TEM).....	51
4.7 Surface properties of Sn doped the mixed metal oxides Catalyst.....	53
CHAPTER V CONCLUSION AND SUGGESTION.....	54
REFERENCES.....	55
APPENDICES.....	60
VITAE.....	71



สถาบันวิทยบริการ
จุฬาลงกรณ์มหาวิทยาลัย

LIST OF FIGURES

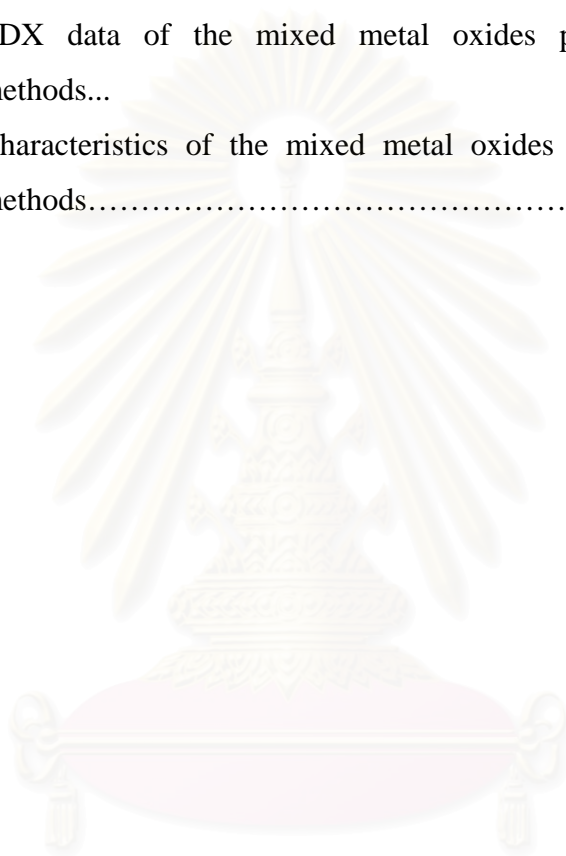
		Page
Figure 2.1	Reflected wave from crystal plane in XRD.....	4
Figure 2.2	Brunauer's five types of adsorption isotherms.....	6
Figure 2.3	Example of an EDX spectrum.....	9
Figure 2.4	SEM image	10
Figure 3.1	Schematic diagrams of the pyrolysis apparatus	17
Figure 4.1	XRD diagrams of single metal oxides and binary oxide of Mg/Zr....	25
Figure 4.2	XRD diagrams of mixed metal oxides of Ni/Mg/Zr prepared by CP method calcined at different temperature (15%Ni, mole ratio Mg/Zr =1, time 6 h.).....	27
Figure 4.3	XRD diagrams of mixed metal oxides of Ni/Mg/Zr prepared by CP method at different time. (15%Ni, mole ratio Mg/Zr =1, calcination temp = 600°C).....	29
Figure 4.4	XRD diagrams of mixed metal oxides of Ni/Mg/Zr prepared by CP method with different Mg/Zr mole ratio (15%Ni, temp. = 600°C, time = 4 h.).....	30
Figure 4.5	Nitrogen adsorption-desorption isotherms of mixed metal oxides of Ni/Mg/Zr prepared by CP method with different mole ratio of Mg/Zr.....	31
Figure 4.6	Pore size distributions of mixed metal oxides of Ni/Mg/Zr prepared by CP method with different Mg/Zr molar ratio.....	32
Figure 4.7	XRD diagrams of mixed metal oxides of Ni/Mg/Zr prepared by CP method with different % wt Ni (mole ratio Mg/Zr =0.25, Temp = 600°C, time = 4 h.).....	33
Figure 4.8	Nitrogen adsorption-desorption isotherms and pore size distributions of mixed metal oxides of Ni/Mg/Zr prepared by CP method with different nickel contents.....	34
Figure 4.9	XRD diagrams of mixed metal oxides of Ni/Mg/Zr prepared by CT method calcined at different temperature (15% wt Ni, mole ratio Mg/Zr =1, time 6 h.).....	35

	Page
Figure 4.10 XRD diagrams of mixed metal oxides of Ni/Mg/Zr prepared by CT method calcined at different time (15%Ni, mole ratio Mg/Zr =1, temp = 800°C).....	37
Figure 4.11 XRD diagrams of mixed oxide of Ni/Mg/Zr prepared by CT method with different Mg/Zr molar ratio (15%Ni, temp = 800°C, time = 4 h.).....	38
Figure 4.12 Nitrogen adsorption-desorption isotherms and pore size distributions of mixed metal oxides of Ni/Mg/Zr prepared by CT method with different Mg/Zr molar ratio.....	39
Figure 4.13 Nitrogen adsorption-desorption isotherms and pore size distributions of mixed metal oxides of Ni/Mg/Zr prepared by CT method with different citric acid content.....	41
Figure 4.14 Nitrogen adsorption-desorption isotherms and pore size distributions of mixed metal oxides of Ni/Mg/Zr prepared by MCT method with different citric acid content.....	43
Figure 4.15 Schematic diagram of the mechanism of formation of mixed metal oxides from citrate precursor.....	44
Figure 4.16 TGA profile of mixed metal oxides of Ni/Mg/Zr prepared from MCP method.....	45
Figure 4.17 Nitrogen adsorption-desorption isotherms and pore size distributions of mixed metal oxides of Ni/Mg/Zr TGA profile of mixed metal oxides of Ni/Mg/Zr prepared by MCT method with different ethylene glycol content.....	47
Figure 4.18 The SEM micrographs of the mixed metal oxides prepared by different methods.....	50
Figure 4.19 The TEM micrographs of the mixed metal oxides prepared by different methods.....	51
Figure 4.20 The TEM micrographs of Sn (0.02 %mole) doped mixed metal oxides of Ni/Mg/Zr prepared by MCT (15%wt Ni, Mg/Zr molar ratio = 0.25, calcination temperature = 800°C, calcinations time = 4 h, citric acid/cation molar ratio =2).....	53

LIST OF TABLES

		Page
Table 3.1	Chemicals and suppliers	16
Table 3.2	Parameters in each method.....	24
Table 4.1	Characteristic XRD patterns of oxides	26
Table 4.2	Characteristics of mixed metal oxides of Ni/Mg/Zr prepared by CP method calcined at different temperature.....	28
Table 4.3	Characteristics of mixed metal oxides of Ni/Mg/Zr prepared by CP method calcined at different time.....	29
Table 4.4	Characteristics of mixed metal oxides of Ni/Mg/Zr prepared by CP method with different Mg/Zr molar ratio.....	30
Table 4.5	Characteristics of mixed metal oxides of Ni/Mg/Zr prepared by CP method with different Mg/Zr molar ratio.....	32
Table 4.6	Characteristics of mixed metal oxides of Ni/Mg/Zr prepared by CP method with different % wt Ni.....	33
Table 4.7	Characteristics of mixed metal oxides of Ni/Mg/Zr prepared by CP method with different % wt Ni.....	35
Table 4.8	Characteristics of mixed metal oxides of Ni/Mg/Zr prepared by CT method at different calcination temperature.....	36
Table 4.9	Characteristics of mixed metal oxides of Ni/Mg/Zr prepared by CT method at different calcination time.....	37
Table 4.10	Characteristics of mixed metal oxides of Ni/Mg/Zr prepared by CT method with different Mg/Zr molar ratio.....	38
Table 4.11	Characteristics of mixed metal oxides of Ni/Mg/Zr prepared by CT method with different Mg/Zr molar ratio (calcined in air at 800°C for 4 h.).....	39
Table 4.13	Characteristics of mixed metal oxides of Ni/Mg/Zr prepared by CT method with different citric acid content.....	42
Table 4.14	Characteristics of mixed metal oxides of Ni/Mg/Zr prepared by MCT method with different citric acid content.....	44

	Page
Table 4.15	Characteristics of mixed metal oxides of Ni/Mg/Zr prepared by MCTE method with different ethylene glycol content (citric acid/total cation molar ratio =2)..... 46
Table 4.16	Optimum conditions in each method 48
Table 4.17	FTIR spectra of mixed metal oxides of Ni/Mg/Zr prepared by different methods..... 48
Table 4.18	EDX data of the mixed metal oxides prepared by different methods... 49
Table 4.19	Characteristics of the mixed metal oxides prepared by different methods..... 52



สถาบันวิทยบริการ
จุฬาลงกรณ์มหาวิทยาลัย

LIST OF SCHEMES

	Page
Scheme 3.1 Coprecipitation method (CP).....	20
Scheme 3.2 Citric acid precursor method (CT).....	21
Scheme 3.3 Modified citric acid precursor method (MCT).....	22
Scheme 3.4 Modified citric acid/ethylene glycol precursor method (MCTE).....	23



สถาบันวิทยบริการ
จุฬาลงกรณ์มหาวิทยาลัย

LIST OF ABBREVIATIONS

XRD	X-ray powder diffraction
SEM	Scanning electron microscopy
BET	Brunauer-Emmett-Teller method
TGA	Thermogravimetric analyzer
FT-IR	Fourier-transform infrared spectroscopy
TEM	Transmission electron microscopy
EDX	Energy dispersive X-ray analysis
CP	Co-precipitation
CT	Citric acid precursor technique
MCT	Modified citric acid precursor technique
MCTE	Modified citric acid and ethylene glycol precursor technique
cm ³	cubic centimeter
wt	weight
h	hour (s)
°C	degree celsius

สถาบันวิทยบริการ
จุฬาลงกรณ์มหาวิทยาลัย

CHAPTER I

INTRODUCTION

1.1 Methane reforming

One of the most important applications of methane is its use in the preparation of synthesis gas. The processes that can produce synthesis gas from methane are steam reforming, CO₂ reforming and partial oxidation. The steam reforming was the dominant commercial method. However, this process has poor selectivity for CO and provides a too high H₂/CO ratio, unsuitable for methanol and Fischer-Tropsch [1,2] syntheses. Compared to steam reforming, the partial oxidation provides very high activity and selectivity, and a suitable CO/H₂ ratio [3,4]. However, although this reaction is only mildly exothermic, a small decrease in the CO selectivity due to the complete combustion of methane, which is a highly exothermic reaction, results in a large increase in the reaction temperature. In addition, a high methane conversion coupled with a high space velocity can produce a large amount of heat in a small region of the catalyst (hot spot). Because it is difficult to remove this heat from the reactor, particularly from a large-scale equipment, the process becomes difficult to control [5].

1.2 Statement of problem

Even though methane conversion to synthesis gas *via* the CO₂ reforming reaction provides a high CO selectivity and a more suitable H₂/CO ratio, it could not be used industrially because of the ageing of the catalyst, caused mainly by carbon deposition. In the CO₂ reforming of CH₄, the carbon deposition sequence for various metals, reported [6] is: Ni >> Pt > Ru. It was reported that carbon deposition cannot be avoided over nickel supported catalysts and for a CO₂/CH₄ molar ratio of 1:1. [7, 14]

The effect of the support on carbon deposition was studied and reported. [8] By replacing Ni with platinum group catalysts, it can suppress the carbon deposition in CO₂ reforming, this provided a CO yield of 69% for Ru and 89% for Ir for a stoichiometric feed of CO₂ and CH₄. [7] It is, however, worthwhile to develop

improved stable and effective nickel-based catalysts, because of the high cost of the noble metals.

Conventionally Ni/MgO catalyst has been prepared by the impregnation method in aqueous solution of nickel salt using MgO support. For MgO, it is synthesized from the decomposition of various magnesium salts [9] which usually results in varied grain sizes, inhomogeneous morphologies and small surface areas, all of which are disadvantages for their use in applications. A modified citric acid precursor technique was used to prepare porous MgO and NiO/MgO nanocomposites with small size and high surface area [10]. Oxalate precursor was also used for preparation of Co-MgO [11].

It was reported that Ni/ZrO₂ catalysts with more than 10 wt% Ni loading showed high activity at 750°C in CO₂ reforming of methane despite producing a large amount of carbon [12]. In addition, Ni/CeO₂-ZrO₂ mixed oxides with Ce/Zr ratio of 0.25 exhibited high activity for methane partial oxidation [13].

As can be seen from above that research on preparing mixed oxides catalysts to get good characteristics is still needed in order to improve their catalytic activity. Therefore, in this work, 4 different methods to prepare mixed oxides catalysts of Ni/Mg/Zr were performed: co-precipitation (CP), citric acid precursor technique (CT), modified citric acid precursor technique (MCT), modified citric acid and ethylene glycol precursor technique (MCTE).

1.3 The objective of the thesis

To synthesize the nickel/magnesium/zirconium mixed oxides catalysts by different methods and to study preparation parameters influencing on the characteristics and properties of the mixed metal oxides catalysts.

1.4 The scope of the thesis

1.4.1 Survey literature.

1.4.2 Synthesize nickel/magnesium/zirconium mixed oxides catalysts by different methods:

- co-precipitation (CP)
- citric acid precursor technique (CT)
- modified citric acid precursor technique (MCT)

- modified citric acid/ethylene glycol precursor technique (MCTE).

The parameters which influencing the properties of the catalysts to be studied are:

Ratio of Mg/Zr	0.25, 1 and 4
Ni content	5-15 %wt of catalysts
Sn content	0.02 mole ratio of Sn/Ni
Calcination time	3-6 h.
Calcination temperature	500, 600, 700 and 800°C

1.4.3 Characterize the prepared catalysts by following methods:

- X-ray diffraction (XRD)
- N₂ adsorption-desorption (BET)
- Transmission electron microscopy (TEM)
- Scanning electron microscopy (SEM)
- Fourier-transform infrared spectroscopy (FT-IR)
- Energy dispersive X-ray analysis (EDX)
- Thermogravimetric analysis (TGA)

1.4.4 Summarize the results and write thesis.

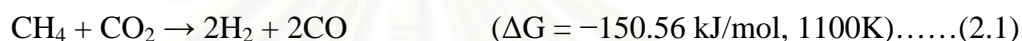
CHAPTER II

THEORY AND LITERATURE REVIEWS

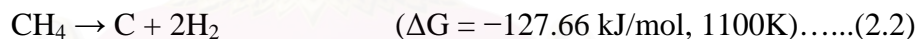
2.1 Theory

2.1.1 Catalytic reforming of methane

Methane reforming with CO₂ (equation 2.1) produces mixture of H₂ and CO with lower H₂/CO ratio than other reforming reactions.



The high endothermic reaction makes it attractive as a choice of media in energy transmission system. Ni was popularly used as the catalyst because of its high activity and low price, but Ni deactivated easily due to coke deposition (mainly from the decomposition of CH₄, in equation 2.2, and metal sintering.



Coke formation is a structure-sensitive process, and depends on the surface. Ni species, particle size, and electron density. A lot of promoters to Ni catalyst and many kinds of supports (oxides, combined-oxides, zeolites, carbon and silicon carbide) were studied in order to eliminate the coke deposition[14,15]. Among the reported promoters, alkali and alkaline earth metals were helpful for the improvement of the coke resistance ability of Ni, while they decreased the reforming activity of the catalysts[16]. Ni/MgO possessed good coke resistance ability due to formation of solid solution Ni-Mg-O[17], but the activity of Ni/MgO is low compared with Ni/Al₂O₃ under the same reaction conditions.

Characterization techniques

2.1.2 X-ray diffraction (XRD)

When the incident x-ray wave hits a crystalline material, it is reflected (mirror-like) as it leaves the crystal planes. The scattering angle (the angle between the original and outgoing rays) is 2θ , see Figure. 2.1.

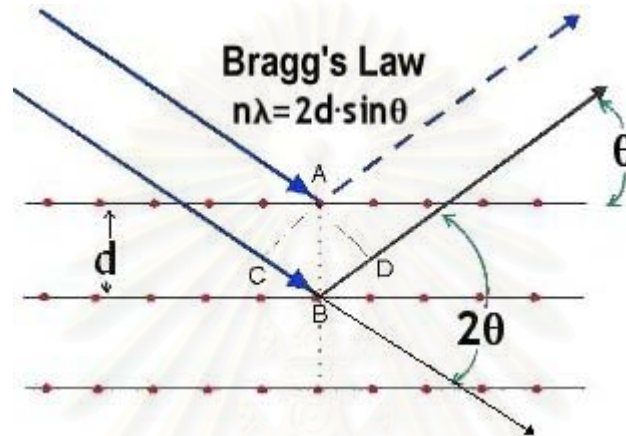


Figure. 2.1 Reflected wave from crystal plane in XRD.

Constructive interference of the reflected waves occurs when this distance is an integral of the wavelength. The *Bragg condition* for the angles of the diffraction peaks is thus [18]:

$$n\lambda = 2d \sin \theta \quad (2.3)$$

where n is the order of diffraction, λ is wavelength of X-ray, d is plane spacing, and θ is Bragg's angle.

The lattice parameters for cubic crystal system and monoclinic crystal system are calculated from the equations 2.4 and 2.5.

Cubic system

$$\sin^2 \theta = \frac{\lambda^2}{4a^2} (h^2 + k^2 + l^2) \quad (2.4)$$

Monoclinic system

$$\sin^2 \theta = \frac{\lambda^2}{4 \sin^2 \beta} \left(\frac{h^2}{a^2} + \frac{k^2 \sin^2 \beta}{b^2} + \frac{l^2}{c^2} - \frac{2hl \cos \beta}{ac} \right) \quad (2.5)$$

The crystallite size was estimated using the Debye-Scherrer equation 2.6.

$$D_{hkl} = 0.9 \lambda / \beta_{hkl} \cos \theta \quad (2.6)$$

Where D_{hkl} is the crystallite size, λ is the wavelength of X-ray, β_{hkl} is the peak width at half maximum and θ is the Bragg diffraction angle.

2.1.3 Brunauer-Emmett-Teller method (BET)

BET is a method for the physical adsorption of gas molecules on a solid surface, found In 1938 by Stephen Brunauer, Paul Hugh Emmett, and Edward Teller. The concept of the theory is an extension of the Langmuir theory, which is a theory for monolayer molecular adsorption, to multilayer adsorption with the following hypotheses: (a) gas molecules physically adsorb on a solid in layers infinitely; (b) there is no interaction between each adsorption layer; and (c) the Langmuir theory can be applied to each layer. The resulting BET equation is expressed by equation 2.7.

$$\frac{1}{v [(P_0/P) - 1]} = \frac{1}{v_m c} \left(\frac{P}{P_0} \right) + \frac{1}{v_m} \quad (2.7)$$

P and P_0 are the equilibrium and the saturation pressure of adsorbates at the temperature of adsorption, v is the adsorbed gas quantity (for example, in volume units), and v_m is the monolayer adsorbed gas quantity. c is the BET constant, which is expressed by equations 2.8.

$$c = \exp \left(\frac{E_1 - E_L}{RT} \right) \quad (2.8)$$

E_1 is the heat of adsorption for the first layer, and E_L is that for the second and higher layers and is equal to the heat of liquefaction.

Equation 2.7 is an adsorption isotherm and can be plotted as a straight line with $1 / v[(P_0 / P) - 1]$ on the y-axis and P / P_0 on the x-axis according to

experimental results. This plot is called a BET plot. The linear relationship of this equation is maintained only in the range of $0.05 < P / P_0 < 0.35$. The value of the slope and the y-intercept of the line are used to calculate the monolayer adsorbed gas quantity v_m and the BET constant c .

A total surface area S_{total} and a specific surface area S are evaluated by the following equations:

$$S_{total} = \frac{(v_m N s)}{M} \quad (2.9)$$

$$S = \frac{S_{total}}{a} \quad (2.10)$$

N : Avogadro's number,

s : adsorption cross section,

M : molecular weight of adsorbate,

a : weight of solid

For adsorption isotherms, there are five principal types, as illustrated in Figure.2.2.

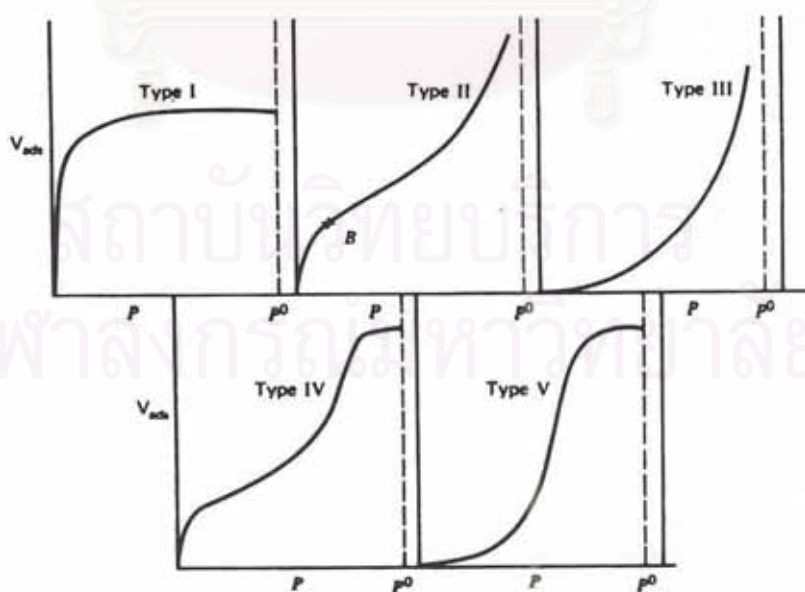


Figure. 2.2 Brunauer's five types of adsorption isotherms.

Type I is the Langmuir type, roughly characterized by a limiting adsorption that presumably corresponds to a complete monolayer.

Type II is very common in the case of physical adsorption and corresponds to multilayer formation. It was the practice to take point *B*, at the knee of the curve, as the point of completion of a monolayer, and surface areas obtained by this method are fairly consistent with those found using adsorbates that give type I isotherms.

Type III is relatively rare, an example is that of the adsorption of nitrogen on ice [20], and seems to be characterized by a heat of adsorption equal to or less than the heat of liquefaction of the adsorbate.

Types IV and V are considered to reflect capillary condensation phenomena in that they level off before the saturation pressure is reached and may show hysteresis effects.

This description is traditional, and some further comment is in order. The flat region of the type I isotherm has never been observed up to pressures approaching P° ; this type typically is observed in chemisorption, at pressures far below P° . Types II and III approach the P° line asymptotically; experimentally, such behavior is observed for adsorption on powdered samples, and the approach toward infinite film thickness is actually due to interparticle condensation [21]. Types IV and V specifically refer to porous solids.

2.1.4 Barrett–Joyner–Halenda method (BJH)

In type IV adsorption isotherms, hysteresis occurs in adsorption and desorption processes. [22] The hysteresis shape depends on the shape of mesopore. Wherever hysteresis exists, equilibrium adsorption amount at desorption is larger than the one at adsorption. This is because capillary condensation of nitrogen gas happens in mesopore and there is difference in meniscus between in adsorption process and in desorption process.

Pore size distribution is calculated from desorption isotherm. Pore curve is expressed as percentage change of pore volume ($\Delta V_p/\Delta r_p$) against micropore radius (r_p). In the area where capillary condensation is in presence, radius of cylinder shaped pore is sum of the thickness of adsorption layer at the arbitrary pressure (t) and pore

radius (r) of meniscus part. Pore size distribution curve can be yielded by plotting $\Delta V/\Delta r$ against pore radius.

$$V_{pn} = R_n \Delta V_n - R_n \Delta t_n c \sum_{j=1}^{n-1} A_{pj} \quad (2.11)$$

V_{pn} : volume of pores

A_p : the area of each pore

R_I : $r_p^2/(r+\Delta t)^2$, r_p =the largest pore radius

2.1.5 Energy Dispersive X-ray analysis (EDX) [23]

Energy Dispersive X-ray analysis (EDX) is sometimes referred to also as EDS or EDAX analysis. It is a technique used for identifying the elemental composition or an area of the specimen. The EDX analysis system works as an integrated feature of a scanning electron microscope (SEM), and cannot operate on its own without the latter.

During EDX analysis, the specimen is bombarded with an electron beam inside the scanning electron microscope. The bombarding electrons collide with the specimen atoms' own electrons, knocking some of them off in the process. A position vacated by an ejected inner shell electron is eventually occupied by a higher-energy electron from an outer shell. To be able to do so, however, the transferring outer electron must give up some of its energy by emitting an X-ray. The amount of energy released by the transferring electron depends on which shell it is transferring from, as well as which shell it is transferring to. Furthermore, the atom of every element releases X-rays with unique amounts of energy during the transferring process. Thus, by measuring the amounts of energy present in the X-rays being released by a specimen during electron beam bombardment, the identity of the atom from which the X-ray was emitted can be established.

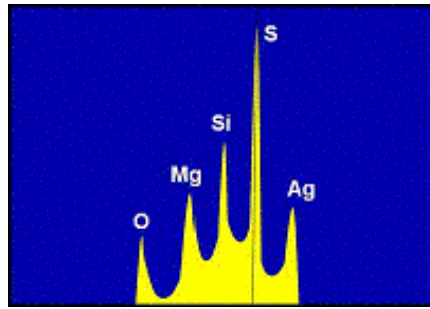


Figure. 2.3 Example of an EDX spectrum.

An EDX spectrum normally displays peaks corresponding to the energy levels for which the most X-rays had been received. Each of these peaks is unique to an atom, and therefore corresponds to a single element. The higher a peak in a spectrum, the more concentrated the element is in the specimen.

2.1.6 Scanning Electron Microscopy (SEM) [24]

Scanning electron microscopy is used for inspecting topographies of specimens at very high magnifications. SEM inspection is often used in the analysis of die/package cracks and fracture surfaces, bond failures, and physical defects on the die or package surface.

During SEM inspection, a beam of electrons is focused on a spot volume of the specimen, resulting in the transfer of energy to the spot. These bombarding electrons, also referred to as primary electrons, dislodge electrons from the specimen. The dislodged electrons, also known as secondary electrons, are attracted and collected by a positively biased grid or detector, and then translated into a signal. To produce the SEM image, the electron beam is swept across the area being inspected, producing many such signals. These signals are then amplified, analyzed, and translated into images of the topography being inspected. Finally, the image is shown on a Cathode Ray Tube (CRT) (Figure. 2.4).

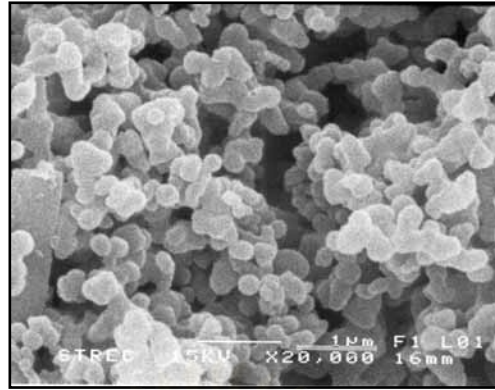


Figure. 2.4 SEM image.

A SEM may be equipped with an EDX analysis system to enable it to perform compositional analysis on specimens. EDX analysis is useful in identifying materials and contaminants, as well as estimating their relative concentrations on the surface of the specimen.

2.1.7 Fourier Transform Infrared Spectroscopy (FTIR)

FTIR is a technique that provides information about the chemical bonding or molecular structure of materials. The technique works on the fact that bonds and groups of bonds vibrate at characteristic frequencies. A molecule that is exposed to infrared rays absorbs infrared energy at frequencies which are characteristic to that molecule. FTIR analysis can also be used for the quantification.

2.1.8 Transmission Electron Microscopy (TEM) [25]

Transmission Electron Microscopy (TEM) is a technique used for analyzing the morphology, crystallographic structure, and even composition of a specimen. TEM provides a much higher spatial resolution than SEM, and can facilitate the analysis of features at atomic scale (in the range of a few nanometers) using electron beam energies in the range of 60 to 350 keV.

Unlike the SEM which relies on dislodged or reflected electrons from the specimen to form an image, the TEM collects the electrons that are transmitted through the specimen. Like the SEM, a TEM uses an electron gun to produce the

primary beam of electrons that will be focused by lenses and apertures into a very thin, coherent beam.

For crystalline materials, the specimen diffracts the incident electron beam, producing local diffraction intensity variations that can be translated into contrast to form an image. For amorphous materials, contrast is achieved by variations in electron scattering as the electrons traverse the chemical and physical differences within the specimen.

2.2 Literature reviews

In 1996, Ruckenstein *et al.* [26] studied the nature of the precursor and the conditions employed to prepare metal supported on MgO catalysts in the CO₂ reforming of methane. Different magnesium precursors were used: Mg(NO₃)₂, Mg(OH)₂, and MgCO₃. Catalytic activities of the catalysts were compared under various conditions. The NiO/MgO catalyst prepared by calcining [MgCO₃]₄Mg(OH)₂ at high temperature for a short time provides the highest conversions of CH₄ and CO₂ and the highest CO yield after 1 h reaction time.

In 2001, Frusteri *et al.* [27] studied the catalytic behavior of the Ni/MgO catalyst in the dry-reforming of methane in the range 575-650°C. The influence of potassium addition has been addressed. Doping of the Ni/MgO catalysts with potassium greatly improves the stability of the catalysts. It was proposed that potassium induced high resistance against coking and sintering phenomena.

In 2002, Potdar *et al.* [28] studied novel one-step co-precipitation/digestion method in the synthesis of stable Ni-Ce-ZrO₂ catalyst. The cubic Ce_{0.8}Zr_{0.2}O₂ catalyst with 15% Ni loading has better activity and thermal stability than impregnated catalyst. These are resulted from the high surface area, the nano-size and the better dispersion of NiO particles in the Ce_{0.8}Zr_{0.2}O₂ matrix and their strong interaction with support material.

In 2003, Valentini *et al.* [29] synthesized Ni nanoparticles in microporous and mesoporous Al and Mg oxides. The oxides have high metal dispersion and good pore size distribution. The β-pinene gas phase hydrogenation proved to be an efficient

catalytic probe for investigating the material's morphological properties. Different pore diameter distributions favored different product selectivities. Lower pore diameters led mainly to isomerization products, while coarser pore diameter distribution promoted mainly hydrogenation products and high β -pinene conversion. However, the dispersion of metal was found to influence the products' selectivity.

In 2003, Guo *et al.* [30] studied a modified sol-gel method to prepare high surface area MgAl_2O_4 spinel. The metal precursors were calcined in flowing air at temperatures (500-900°C). PVA (polyvinyl alcohol) was used as polymerizing agent and ammonium as pH regulator. The amount of PVA significantly affects the surface area of the samples. With increasing the ratio of metal/PVA, the surface area of the resulting spinels increased.

In 2003, Bouarab *et al.* [31] studied the dry-reforming of methane to syngas on the series of Co/SiO_2 catalysts modified by MgO (5-35 wt.%) in the temperature range of 500-800°C. It was demonstrated that very positive effects on catalyst stability arise from the formation of a magnesium silicate phase for a tuned amount of MgO additive. This phase prevents cobalt phase sintering by avoiding particle coalescence. This bi-functional process hinders deactivating carbon formation: (i) by limiting bulk cobalt carbide and therefore carbon filament formation, which may lead to reactor plugging and/or particle fragmentation, and (ii) by suppressing encapsulating carbon formation which limits access of reactant to the active cobalt phase.

In 2004, Song *et al.* [32] studied catalytic dry-reforming of methane using metal loaded on several supports. Catalytic activities are in the order of $\text{Ni/MgO} > \text{Ni/MgO/CeZrO}_2 > \text{Ni/CeO}_2 \approx \text{Ni/ZrO}_2 \approx \text{Ni/Al}_2\text{O}_3 > \text{Ni/CeZrO}_2$. High CH_4 conversion (~97%) and high CO_2 conversion (around 80%) were obtained with H_2/CO ratios of 1.5–2.0, at 800–850°C under atmospheric pressure. The catalysts showed less carbon formation. The higher CO_2 conversion over Ni/MgO and Ni/MgO/CeZrO_2 may be related to the stronger interaction of CO_2 with MgO and more interface between Ni and MgO resulting from the formation of NiO/MgO solid solution.

In 2004, GuO *et al.* [33] studied the dry reforming of methane to synthesis gas over Ni catalysts supported over various supports, γ -Al₂O₃, MgO- γ -Al₂O₄, and MgAl₂O₄ by the co-precipitation method. Compared to Ni/ γ -Al₂O₃, the Ni/MgO- γ -Al₂O₃ and Ni/MgAl₂O₄ catalysts exhibit higher activity and better stability using a stoichiometric feed ratio (1:1). The MgAl₂O₄ spinel layer in Ni/MgO- γ -Al₂O₃ can effectively suppress the phase transformation to form NiAl₂O₄ spinel phases and can stabilize the Ni tiny crystallites, to which the good stability of the catalyst contributes. The high sintering-resistance ability and low acidity of MgAl₂O₄ compared to γ -Al₂O₃ and the interactions between Ni and MgAl₂O₄ might be responsible for its high activity and resistant to coking and sintering.

In 2004, Chen *et al.* [34] prepared nanoporous MgO and NiO/MgO nanocomposites by a modified citrate method. They have high surface area and controlled particle size. The average particle size of products can be manipulated in the range of 5–20 nm by controlling the ratio of citric acid to metal cations and the annealing temperature. TEM shows that there are many big pores on the surface of the agglomerations; these pores contribute to high surface area (230 m²/g).

In 2004, Montemayor *et al.* [35] reported preparation and characterization of cobalt ferrite by the polymerized complex method. Metal precursor solutions were mixed with citric acid (CA), ethylene glycol (EG) in a molar ratio of Co/Fe/CA/EG=1/2/9/22.5 at 130°C. Two types of reactions were formed: the formation of metal-CA complexes and successive esterification reactions between CA and EG. Controlled thermal treatments between 400 and 700°C of the resin allowed obtaining nanoparticles of pure CoFe₂O₄. The powders obtained presented a ferrimagnetic behavior.

In 2004, Roh *et al.* [36] studied carbon dioxide reforming of methane over co-precipitated Ni–CeO₂, Ni–ZrO₂ and Ni–Ce–ZrO₂ catalysts. Two metal loading methods were compared. The ZrO₂ support provides more stable catalysts than CeO₂. The co-precipitation method is more effective to prepare highly active and stable Ni–CeO₂ and Ni–Ce–ZrO₂ catalysts than the impregnation method. The catalyst prepared by co-precipitation has higher BET surface area and smaller crystallite sizes. The Ni–Ce–ZrO₂ catalyst exhibits high activity and stability at 800°C.

In 2004, Hou *et al.* [37] studied surface properties of a coke-free Sn doped nickel catalyst for the CO₂ reforming of methane. The characterization was performed using H₂-TPR, FE-SEM, and FE-TEM analysis. The results indicated that Sn improved the dispersion of Ni and retarded the sintering of active Ni particles during the reaction. Surface enrichment of Sn made a large portion of the Ni surface covered by these promoters and hindered the access of CH₄ and/or CO₂ on the surface of Ni particles.

In 2005, Mariappan *et al.* [38] synthesized nanostructured LiTi₂(PO₄)₃ powder by the polymerized complex method. The method is based on the formation of highly water-soluble precursors to avoid the use of alkoxides. A pure phase of LiTi₂(PO₄)₃ powder was obtained when molar ratio of ethylene glycol/citric acid = 1. Calcination temperatures were varied from 650 to 1050°C. Both XRD and TEM showed that nanostructured particles of 50 nm are formed at 650°C.



สถาบันวิทยบริการ
จุฬาลงกรณ์มหาวิทยาลัย

CHAPTER III

EXPERIMENTAL

3.1 Chemicals

All chemicals used were analytical grade, and obtained as listed in Table 3.1.

Table 3.1 Chemicals and suppliers

Chemicals	Suppliers
Nickel(II) nitrate hexahydrate	CARLO
Magnesium nitrate hexahydrate	Fluka Chemie A.G., Switzerland
Zirconyl nitrate hydrate	CARLO
Citric acid monohydrate	Fluka Chemie A.G., Switzerland
Ethylene glycol	Fluka Chemie A.G., Switzerland
Stannous chloride dihydrate	Fluka Chemie A.G., Switzerland
Ethanol	Merck, Germany
Ultra high purity nitrogen gas (99.99%)	Thai Industry Gas Co., Ltd., Thailand

สถาบันวิทยบริการ
จุฬาลงกรณ์มหาวิทยาลัย

3.2 Equipment and apparatus

Oven and furnace

The catalysts were preliminary dried at 120-200°C in a Memmert UM-500 oven and further calcined at 500-950°C in a Carbolite RHF 1600 muffle furnace with programmable heating rate of 3°C/min.

Pyrolysis apparatus

In some preparative methods, the step of heating oxides was performed using the pyrolysis apparatus assembled in laboratory which comprises a quartz tubular reactor of 10-mm. inner diameter, shown in Figures 3.1. The samples were heated at 800°C in N₂.

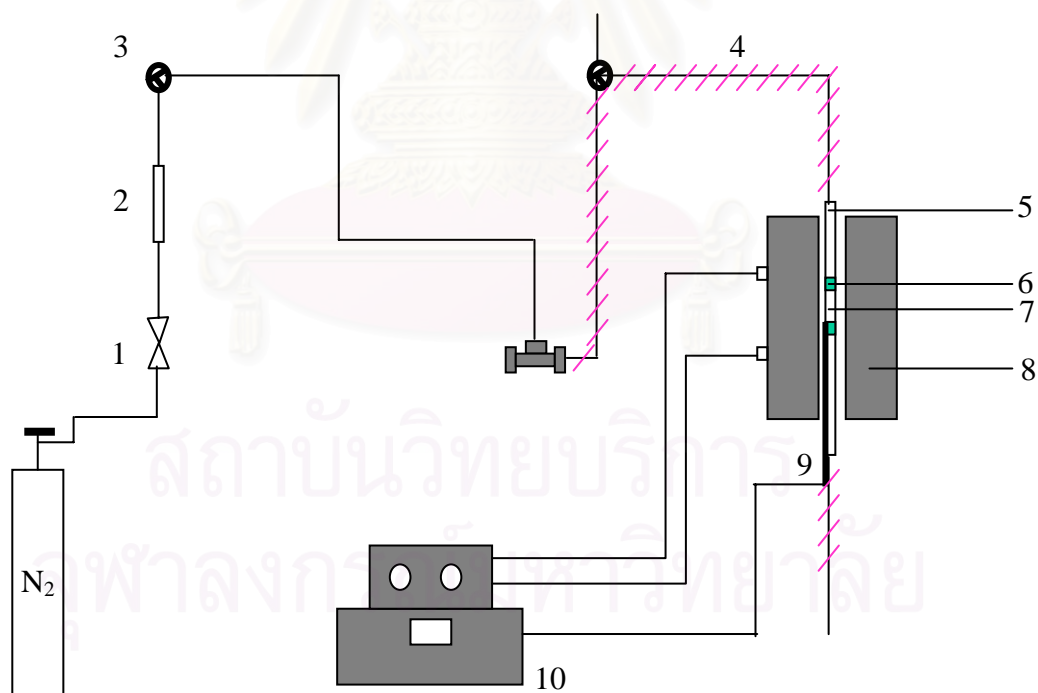


Figure 3.1 Schematic diagrams of the pyrolysis apparatus.

- | | | |
|--|-----------------------|----------------------|
| 1 = needle valve, | 2 = flow controller, | 3 = three-way valve, |
| 4 = heater cable, | 5 = tubular reactor, | 6 = quartz wool, |
| 7 = catalyst, | 8 = electric furnace, | 9 = thermocouple, |
| 10 = temperature programmed controller | | |

3.3 Characterization methods

3.3.1 Fourier-transform infrared spectroscopy (FT-IR)

Fourier-transform infrared spectra were recorded on Nicolet FT-IR Impact 410 Spectrophotometer. The samples were made into a KBr pellet. Infrared spectra were recorded between 400 to 4000 cm^{-1} in transmittance mode.

3.3.2 X-ray powder diffraction (XRD)

The XRD patterns were obtained on Rigaku, DMAX 2002/Ultima Plus. X-ray diffraction is used to obtain information about the structure and composition.

3.3.3 Nitrogen adsorption (Brunauer-Emmett-Teller method (BET))

BET specific surface area of the catalysts was carried out using a BELSORP-mini. The principle of this method is by adsorption of a particular molecular species from a gas or liquid onto the surface. Based upon one adsorbed layer, the quantity of adsorbed material gave directly the total surface area of the sample. The pore size distributions were obtained according to the Barret–Joyner–Halenda (BJH) method from the adsorption branch data.

3.3.4 Transmission electron microscopy (TEM)

TEM was performed with a JEOL JEM-2010F machine equipped with a Gatan slow-scan camera for high-resolution observation. The accelerating voltage applied was 200 kV. Specimens for TEM were prepared by standard techniques. Element composition of TEM specimens was measured by registering an emission of X-rays from specimen with an attached Link ISIS energy dispersive X-ray spectrometer (EDS).

3.3.5 Scanning Electron Microscopy (SEM)

SEM was performed with JEOL JEM-6400 for the surface investigation. A Zygo NewView5000 white light interferometer (WLI) with a 50 objective and 0.4 zoom magnifications provided surface profiles to quantify the surface microroughness.

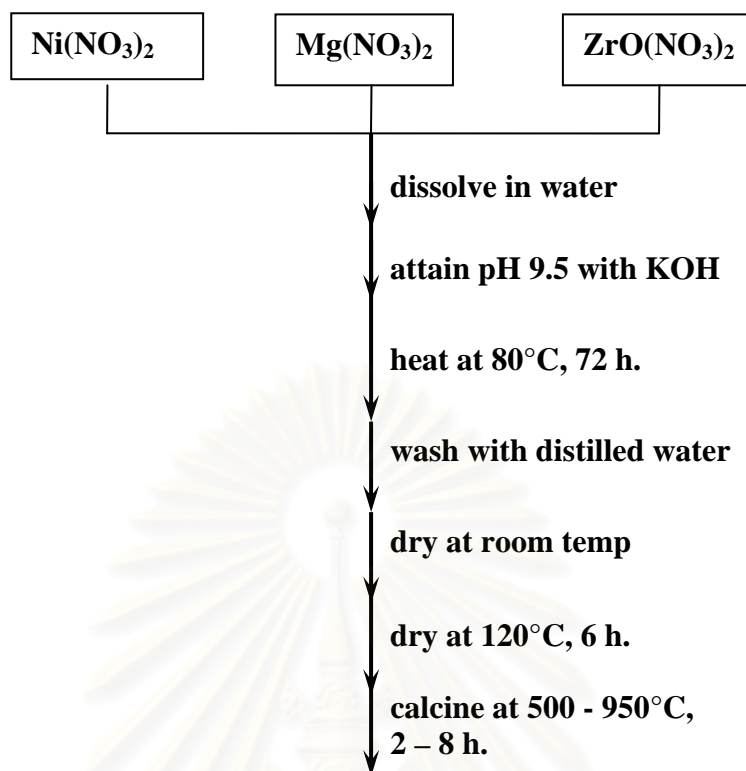
3.3.6 Thermogravimetric Analyzer (TGA)

TGA involves heating a sample in an inert or oxidizing atmosphere and measuring the weight. The weight change over specific temperature ranges provides indications of the composition of the sample and thermal stability. Measurement of the residue mass of substances according to a controlled temperature program was made using Netzsch STA 409 thermobalance of TA Instruments with an increment of 20°C /min. heating rate under a N₂ flow of 20 cm³/min.

3.4 Synthesis of mixed metal oxides of Ni/Mg/Zr

A. Coprecipitation method (CP)

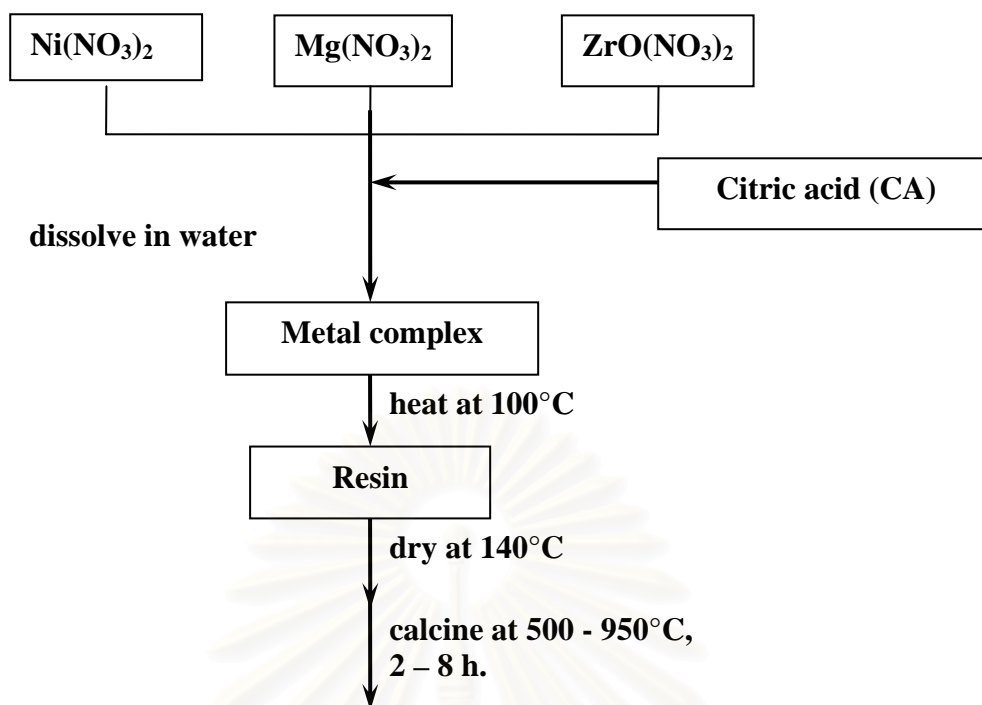
Nickel (II) nitrate hexahydrate (0.74 g), magnesium nitrate hexahydrate (0.56 g), zirconyl nitrate hydrate (2.96 g), were dissolved in water, and the resulting solution was added aqueous solution of KOH (20 % w/w) drop-wise at 80°C. The pH was maintained at 9.5. The precipitates were digested at 80°C for 72 h. Then they were thoroughly washed with distilled water and dried at room temperature for 2 days. And then they were dried again at 120°C for 6 h. The dried mass thus obtained was finely ground and calcined in air at various temperatures and time.



Scheme 3.1 Coprecipitation method (CP)

B. Citric acid precursor method (CT)

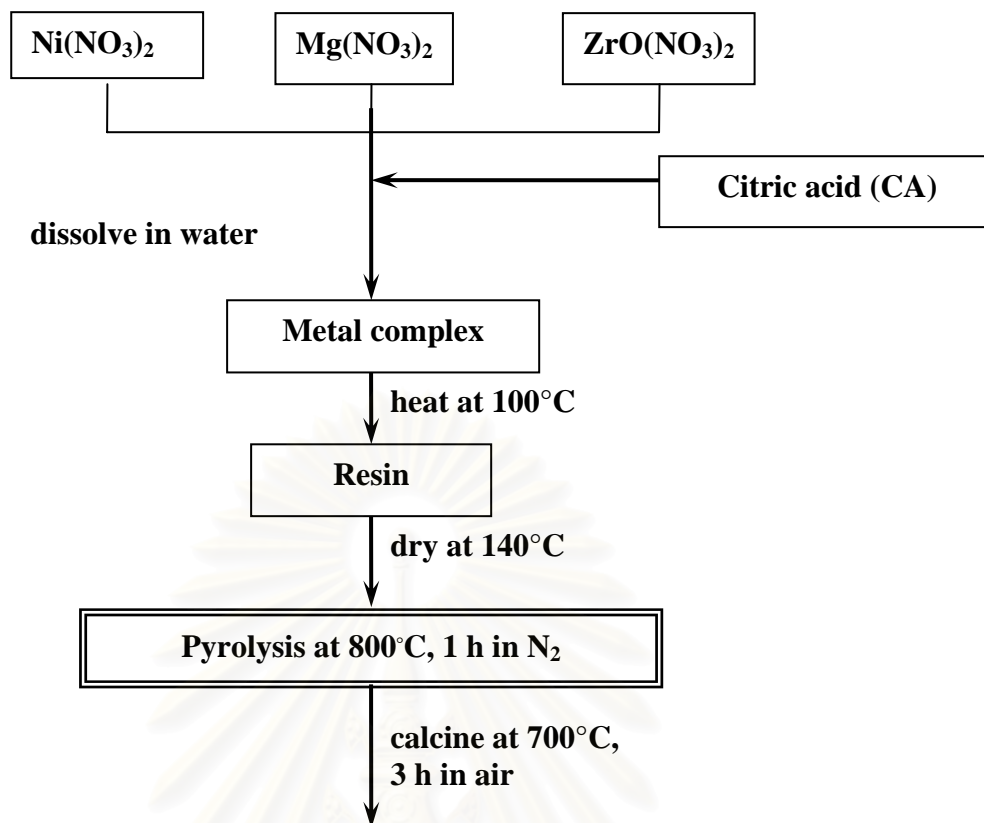
Nickel (II) nitrate hexahydrate (0.74 g), magnesium nitrate hexahydrate (0.56 g), zirconyl nitrate hydrate (2.96 g), were dissolved in 50 ml deionized water. Then citric acid (5.18 g) was added. After 10 minutes stirring, the solution became clear; the solution was then heated on a magnetic stirrer to evaporate the water. During the procedure of evaporation, the solution becomes thicker and thicker. Half an hour later, a viscous state was reached. Then the beaker was moved to an oven with a temperature of 140°C for 1 h. The gel was dried to get a fluffy powder which then it was calcined in air at various temperatures and time.



Scheme 3.2 Citric acid precursor method (CT).

C. Modified citric acid precursor method (MCT)

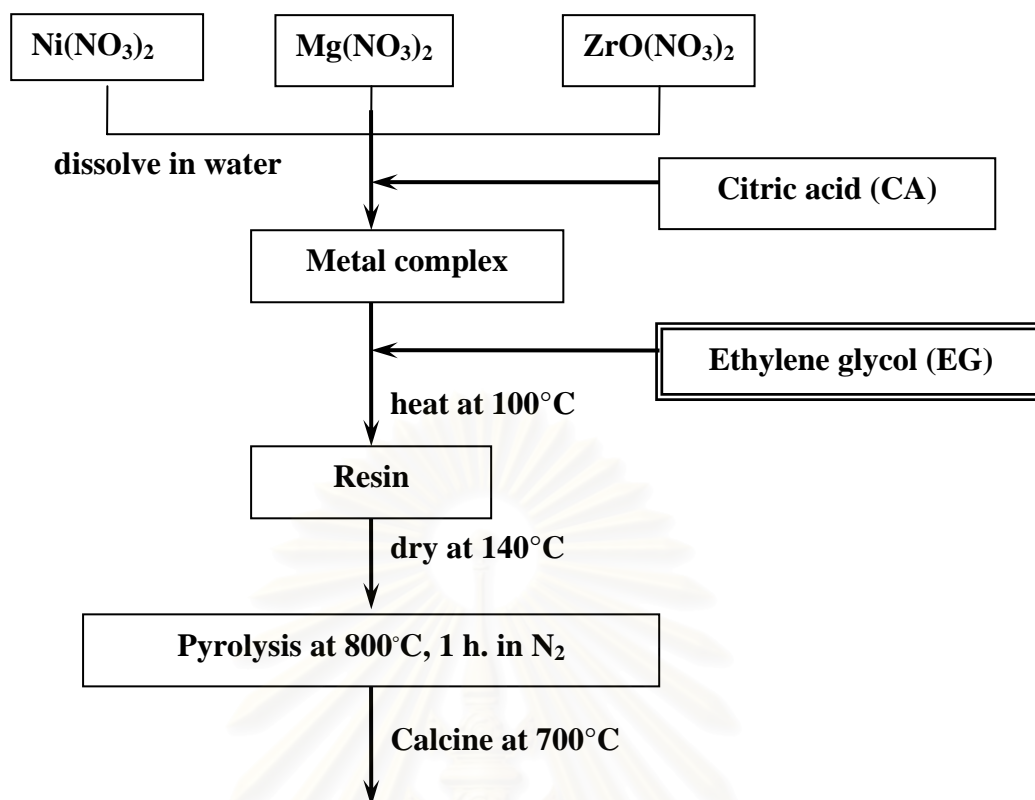
The preparation follows the method B except in the step of powder calcination. The gel was dried to get a fluffy powder which then was calcined at 800°C for 1 h in nitrogen, then further calcined at 700°C for 3 h in air to remove carbon and get mixed oxide crystals. In an attempt to control the grain size of the oxides, experiments were conducted by varying the ratio of the citric acid to the cation and the calcination temperatures.



Scheme 3.3 Modified citric acid precursor method (MCT).

D. Modified citric acid and ethylene glycol precursor method (MCTE)

The preparation follows C except that ethylene glycol (7.77 g) was also added, following the addition of citric acid. Then the contents were heated at 100°C to evaporate water and heated at 800°C in N_2 to get an amorphous mixture with mixed oxide and carbon. The mixture then was calcined in air at 700°C for 3 h. to remove carbon and get mixed oxide crystals.



Scheme 3.4 Modified citric acid/ethylene glycol precursor method (MCTE).

Table 3.2 Parameters used in each method

Parameters	CP	CT	MCT	MCTE
Calcination temperature ($^\circ\text{C}$)	500-950	500-950	800	800
Calcination time	2-8	2-8	4	4
Mg/Zr molar ratio	0.25-4	0.25-4	1	1
% Ni	5-15	15	15	15
Citric acid/metal molar ratio	-	1-2	1-2	-
Citric acid/ethylene glycol molar ratio	-	-	-	1-2

E. Sn doping

In the experiment with Sn doping in order to see effect of Sn on morphology of the mixed oxides, the preparation follows C except that stannous chloride dihydrate (0.01 g, 0.02% mole) was also added following the addition of citric acid. Then the contents were heated at 100°C to evaporate water and heated at 800°C in N₂. The mixture was then calcined in air at 700°C for 3 h.

3.5 Synthesis of single metal oxide

In this work, single metal oxides: NiO, MgO and ZrO₂ were also prepared in order to compare with the mixed metal oxides, the coprecipitation method (CP) was used. Metal nitrate: nickel (II) nitrate hexahydrate, magnesium nitrate hexahydrate or zirconyl nitrate hydrate was dissolved in water, and the resulting solution was added aqueous solution of KOH (20 % w/w) drop-wise at 80°C. The pH was maintained at 9.5. The precipitates were digested at 80°C for 72 h. Then they were thoroughly washed with distilled water, dried, ground and calcined in air at 600°C.

CHAPTER IV

RESULTS AND DISCUSSION

In this work, the mixed oxides catalysts of Ni/Mg/Zr were prepared by 4 different methods:

1. Co-precipitation (CP)
2. Citric acid precursor technique (CT)
3. Modified citric acid precursor technique (MCT)
4. Modified citric acid and ethylene glycol precursor technique (MCTE)

The resultant catalysts were characterized by XRD, FT-IR, SEM, TEM, BET and TGA techniques.

4.1 Single metal oxides and binary oxide of Mg/Zr

For comparison, oxide of each single metal (Mg, Zr, Ni) and binary mixed oxide (Mg/Zr) were prepared by coprecipitation method. Their X-ray diffraction patterns were shown in Fig. 4.1. Characteristic peaks are summarized in Table 4.1.

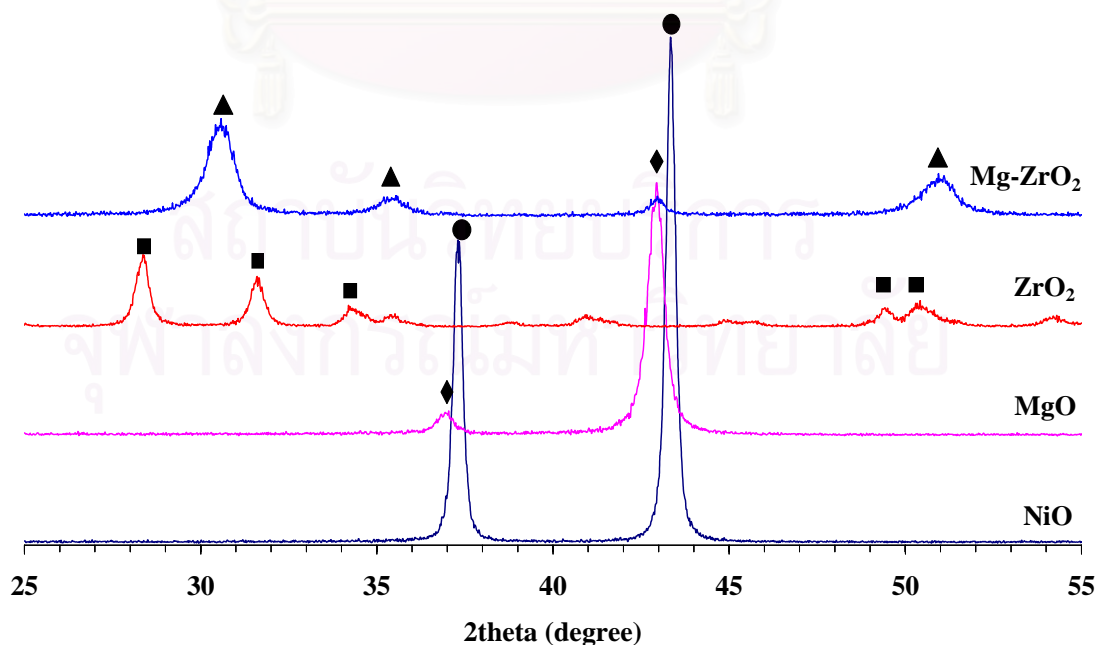


Figure 4.1 XRD diagrams of single metal oxides and binary oxide of Mg/Zr.

Table 4.1 Characteristic XRD patterns of oxides.

Oxide	2θ	d-spacing (nm)	Miller indices
NiO	37.1	0.24218	(111)
	43.1	0.20973	(200)
MgO	37.0	0.24301	(111)
	43.0	0.21045	(200)
ZrO ₂	28.2	0.31627	(-111)
	31.5	0.28392	(111)
	34.4	0.26048	(020)
	49.3	0.18477	(022)
	50.1	0.18181	(220)
Mg-ZrO ₂	30.6	0.29289	(111)
	35.4	0.25365	(200)
	50.9	0.17936	(220)

Each single metal oxide showed its characteristic XRD pattern. NiO and MgO are face-centered-cubic oxides with very close lattice parameters (4.196 and 4.212 Å for NiO and MgO, respectively) and bond distances (2.10 and 2.11 Å for NiO and MgO, respectively). The results are in good agreement with the XRD patterns of each metal oxide (NiO, JCPDS: 65-2901; MgO, (JCPDS: 77-2364; ZrO₂, JCPDS: 86-1449; and Mg-ZrO₂, JCPDS: 77-2156).

The XRD diffractograms show that the mixed metal oxide exist as Mg-ZrO₂ phase ($2\theta = 30.6, 35.4, 50.9$). It can be seen that the reflections are shifted from those of the MgO and ZrO₂, this corresponds to cubic Mg-ZrO₂ solid solution with the lattice parameter of 5.09 Å.

4.2. Mixed metal oxides of Ni/Mg/Zr prepared by co-precipitation (CP)

4.2.1 Effect of calcination temperature

Temperature is an important function to catalyst phase changing. Figure 4.2 shows XRD diagrams of mixed oxides of Ni/Mg/Zr, Mg/Zr molar ratio = 1, 15% wt Ni calcined at different temperature. The calcination time is fixed at 6 h.

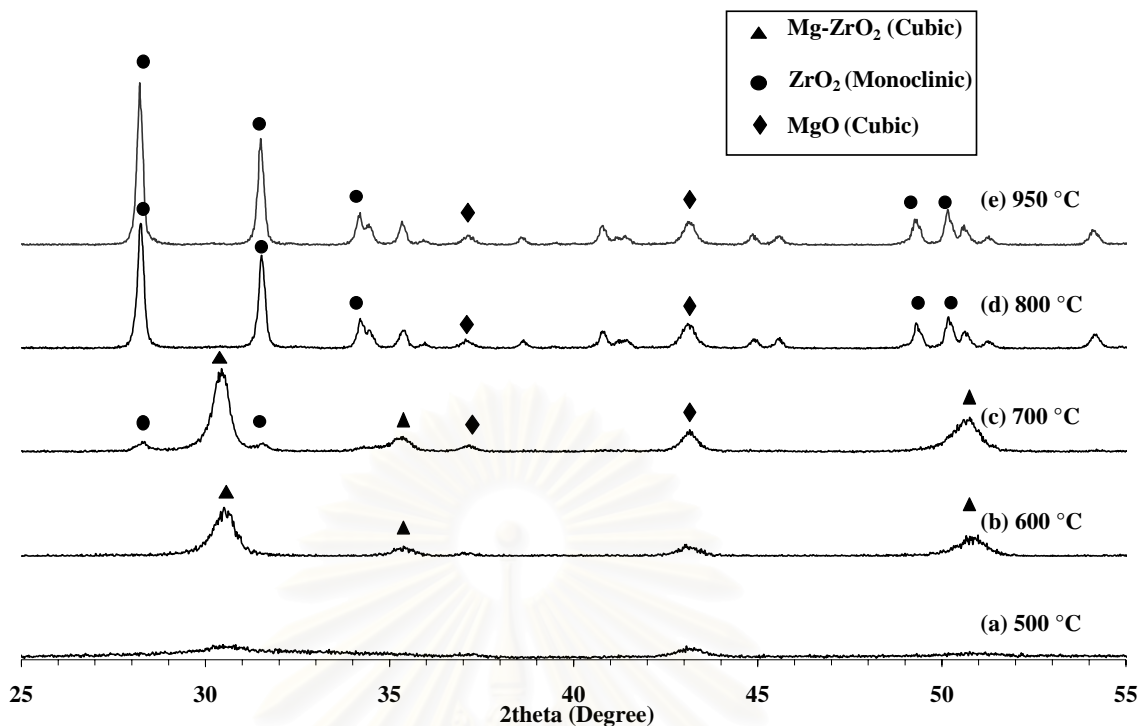


Figure 4.2 XRD diagrams of mixed metal oxides of Ni/Mg/Zr prepared by CP method calcined at different temperature (15% wt Ni, mole ratio Mg/Zr =1, time = 6 h.).

The result of phase change from XRD showed that at calcination temperature around 600-700°C, only one phase was present. Peak matching with the XRD library data revealed that this phase is Mg-ZrO₂ ($2\theta = 30.6, 35.4, 50.9, 60.5, 63.5$). When the calcination temperature was increased to 800-950°C, ZrO₂ monoclinic phase (JCPDS: 86-1449, $2\theta = 28.2, 31.5, 34.4, 49.3, 50.1$) was present together with small amount of MgO.

For the crystallite sizes, they were determined by XRD diffraction maximum from the half-width of diffraction peaks using Scherrer's formula [18]. The sizes were calculated on the (111) plane for Mg-ZrO₂ phase and (-111) for ZrO₂ phase. The data on crystallite size and unit cell parameters are listed in Table 4.2.

Table 4.2 Characteristics of mixed metal oxides of Ni/Mg/Zr prepared by CP method calcined at different temperature

Calcination temperature (°C)	Crystallite size (nm)	Phase	Unit cell parameters (Å)		
			a	b	c
500	15	Mg-ZrO ₂ cubic	5.09	5.09	5.09
600	14	Mg-ZrO ₂ cubic	5.09	5.09	5.09
700	17	Mg-ZrO ₂ cubic	5.08	5.08	5.08
800	44	ZrO ₂ monoclinic MgO	5.14	5.2	5.31
950	51	ZrO ₂ monoclinic MgO	5.14	5.2	5.31

The Mg-ZrO₂ crystallites show cubic pattern with unit cell dimension of 5.09 Å. When the calcined temperature was increased to 800°C, the crystal structure was changed into monoclinic with unit cell dimension of 5.14 (a), 5.20 (b), 5.31 (c) Å.

From the result obtained, it showed that the optimum calcination temperature is at 600°C as only Mg-ZrO₂ phase was detected.

4.2.2 Effect of calcination time

Mixed metal oxides of Ni/Mg/Zr, Mg/Zr molar ratio =1, with 15% wt Ni were calcined at 600°C on different time. XRD patterns are shown in Figure 4.3.

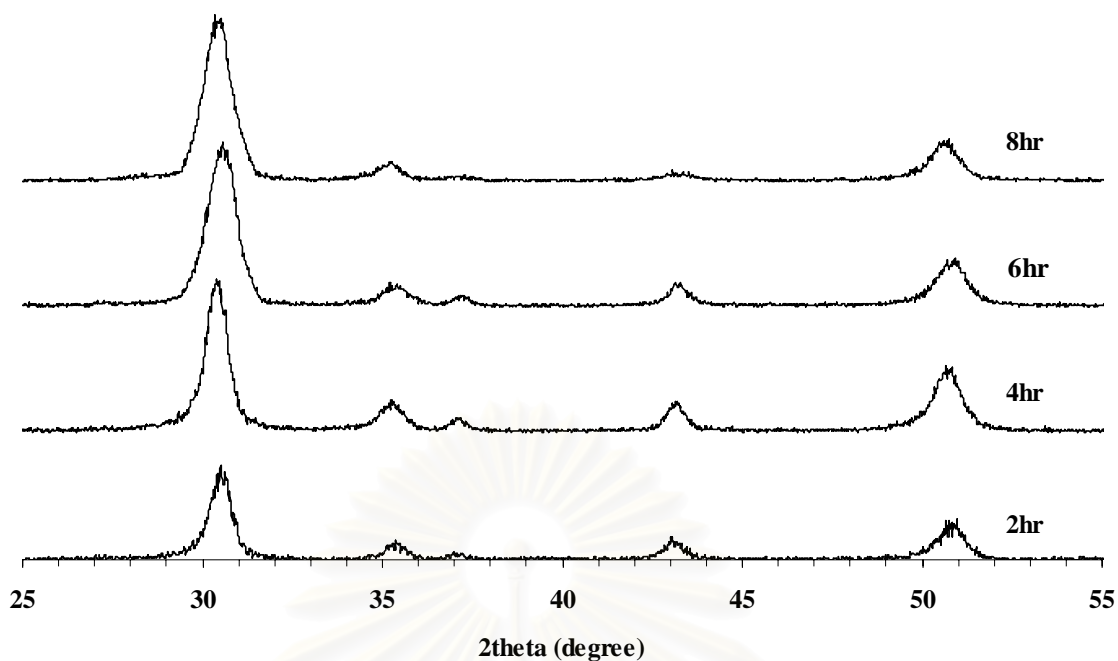


Figure 4.3 XRD diagrams of mixed metal oxides of Ni/Mg/Zr prepared by CP method at different calcination time. (15% wt Ni, Mg/Zr molar ratio =1, calcination temp = 600°C).

It can be seen that the peak widths decrease a little when the time increased. No significant change in peak intensity was observed after 4 h.

From the peak intensity, the relative crystallinity of the oxides can be calculated and it is listed in Table 4.3. Calcination time of 4 h gives higher % crystallinity, so the optimum calcination time is 4 h. The crystallite size is not affected by the calcination time.

Table 4.3 Characteristics mixed metal oxides of Ni/Mg/Zr calcined prepared by CP method at different time

Calcination time (h)	Relative crystallinity (%)	Crystallite size (nm)	Lattice parameter of Mg-ZrO ₂ (Å)
2	71	13	5.08
4	100	13	5.09
6	99	14	5.09
8	99	15	5.09

4.2.3 Effect of Mg/Zr molar ratio

XRD patterns of the mixed metal oxides of Ni/Mg/Zr with different Mg/Zr molar ratio, 15% wt Ni using calcination temperature of 600°C and calcination time = 4 h are shown in Figure 4.4. The relative crystallinity, crystalline size and lattice parameter are listed in Table 4.4.

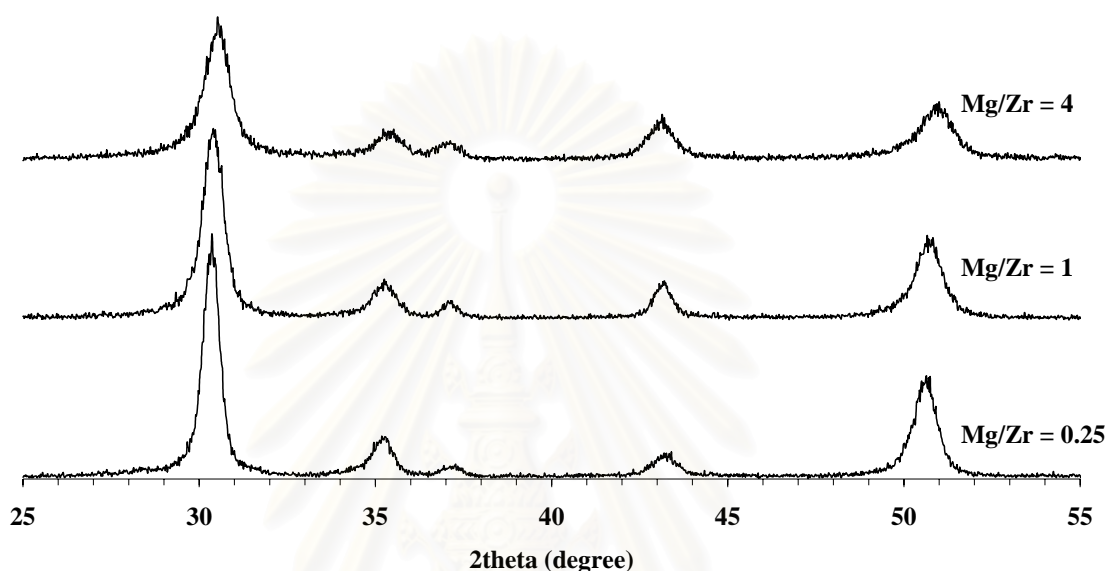


Figure 4.4 XRD diagrams of mixed metal oxides of Ni/Mg/Zr prepared by CP method with different Mg/Zr molar ratio (15% wt Ni, temp = 600°C, time = 4 h).

Table 4.4 Characteristics of mixed metal oxides of Ni/Mg/Zr prepared by CP method with different Mg/Zr molar ratio

Mg/Zr Mole ratio	Relative crystallinity (%)	Crystallite size (nm)	Lattice parameter of Mg-ZrO ₂ (Å)
0.25	100	17	5.09
1	82	13	5.09
4	63	12	5.08

The peak widths increased when Mg/Zr molar ratio was increased (that is higher Mg content). This resulted in smaller crystallite size.

The peak intensity decreased when Mg/Zr molar ratio increased. This resulted in lower %crystallinity.

From the results obtained, it is shown that the crystallite size and % crystallinity can be controlled by changing molar ratio of Mg/Zr.

Another important characteristic of catalyst is surface area and pore size, so in this work, the surface area is determined by BET. N₂ adsorption–desorption isotherm for the Ni/Mg/Zr mixed oxides with different Mg/Zr molar ratio are shown in Figure 4.5. The pore size distributions were obtained according to the Barrett–Joyner–Halenda (BJH) method using the Halsey equation for multilayer thicknesses, shown in Figure 4.6. The data are tabulated in Table 4.5.

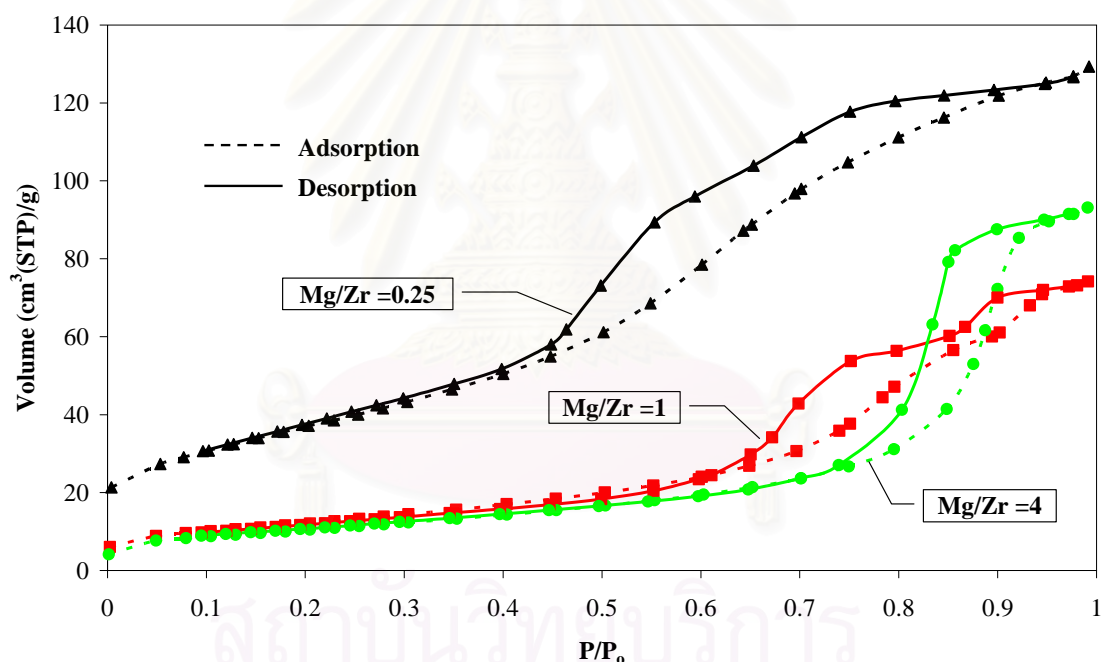


Figure 4.5 Nitrogen adsorption-desorption isotherms of Ni/Mg/Zr mixed oxide prepared by CP method with different Mg/Zr molar ratio.

From BET isotherms, they match with type IV with hysteresis effect. Absorption and evaporation of gas occurred from condensation that evaporated on small pore size catalyst. The small pore size is from hysteresis effect.

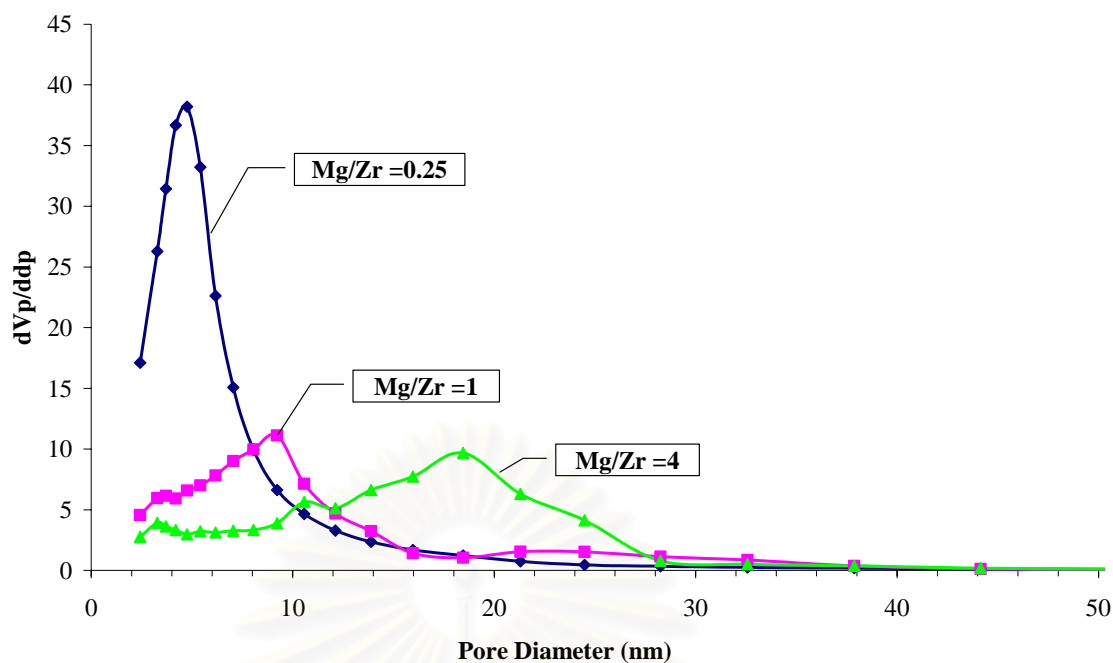


Figure 4.6 Pore size distributions of mixed metal oxides of Ni/Mg/Zr prepared by CP method with different Mg/Zr molar ratio.

The pore size distribution obtained when Mg/Zr molar ratio = 0.25 is narrower than that with molar ratio of 1 and 4. This means that the dispersion of pore is homogeneous.

Surface area, pore volume and average pore size of the mixed metal oxides are presented in Table 4.5.

Table 4.5 Characteristics of mixed metal oxides of Ni/Mg/Zr prepared by CP method with different Mg/Zr molar ratio

Mg/Zr Molar ratio	Surface area (m ² /g)	Pore volume (cm ³ /g)	Average pore size (nm)
0.25	136	0.20	5.9
1	45	0.11	10.2
4	38	0.14	15.0

From the data, the highest surface area of Mg/Zr is obtained at Mg/Zr molar ratio = 0.25. The pore size is in the range of mesopore (2-50 nm).

4.2.4 Effect of % wt Ni

XRD patterns of the mixed metal oxides of Ni/Mg/Zr ($Mg/Zr = 0.25$) with different % wt Ni calcined in air at $600^{\circ}C$ for 4 h. are shown in Figure 4.7.

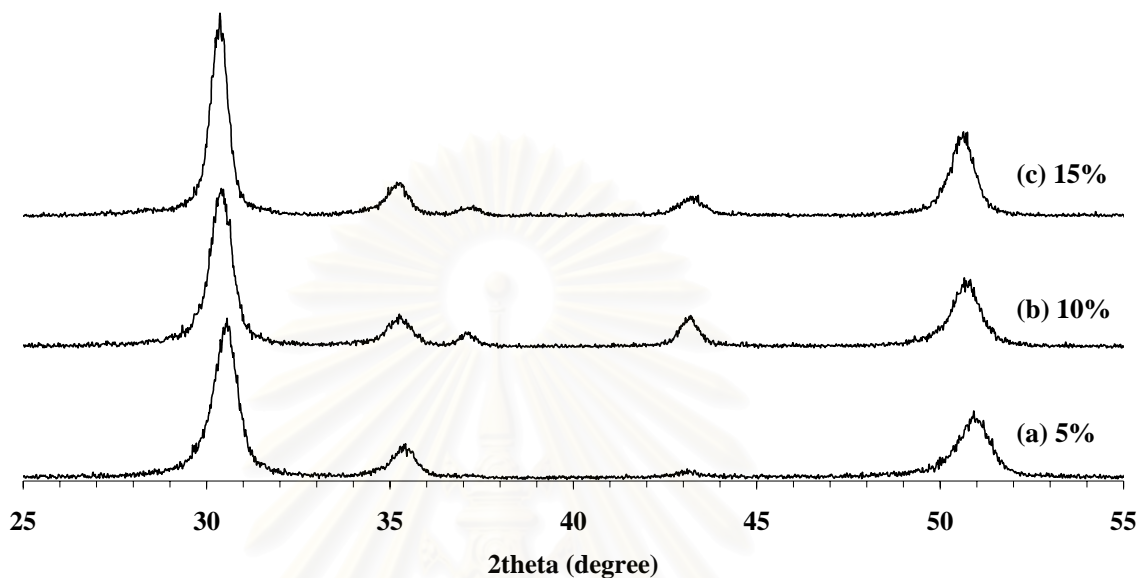


Figure 4.7 XRD diagrams of mixed metal oxides of Ni/Mg/Zr prepared by CP method with different % Ni (mole ratio $Mg/Zr = 0.25$, Temp = $600^{\circ}C$, time = 4 h.).

It can be seen that %wt Ni has no effect on both crystallite size and % crystallinity.

Table 4.6 Characteristics of mixed metal oxides of Ni/Mg/Zr prepared by CP method with different % wt Ni

% wt Ni	Relative crystallinity (%)	Crystallite size (nm)	Lattice parameter of Mg-ZrO ₂ (Å)
5	100	13	5.06
10	100	12	5.07
15	100	12	5.08

N₂ adsorption–desorption isotherm and the pore size distributions obtained for the Ni/Mg/Zr mixed oxides with different % wt nickel, are shown in Figure 4.8.

Surface area, pore volume and average pore size of the mixed metal oxides with different nickel content are presented in Table 4.7.

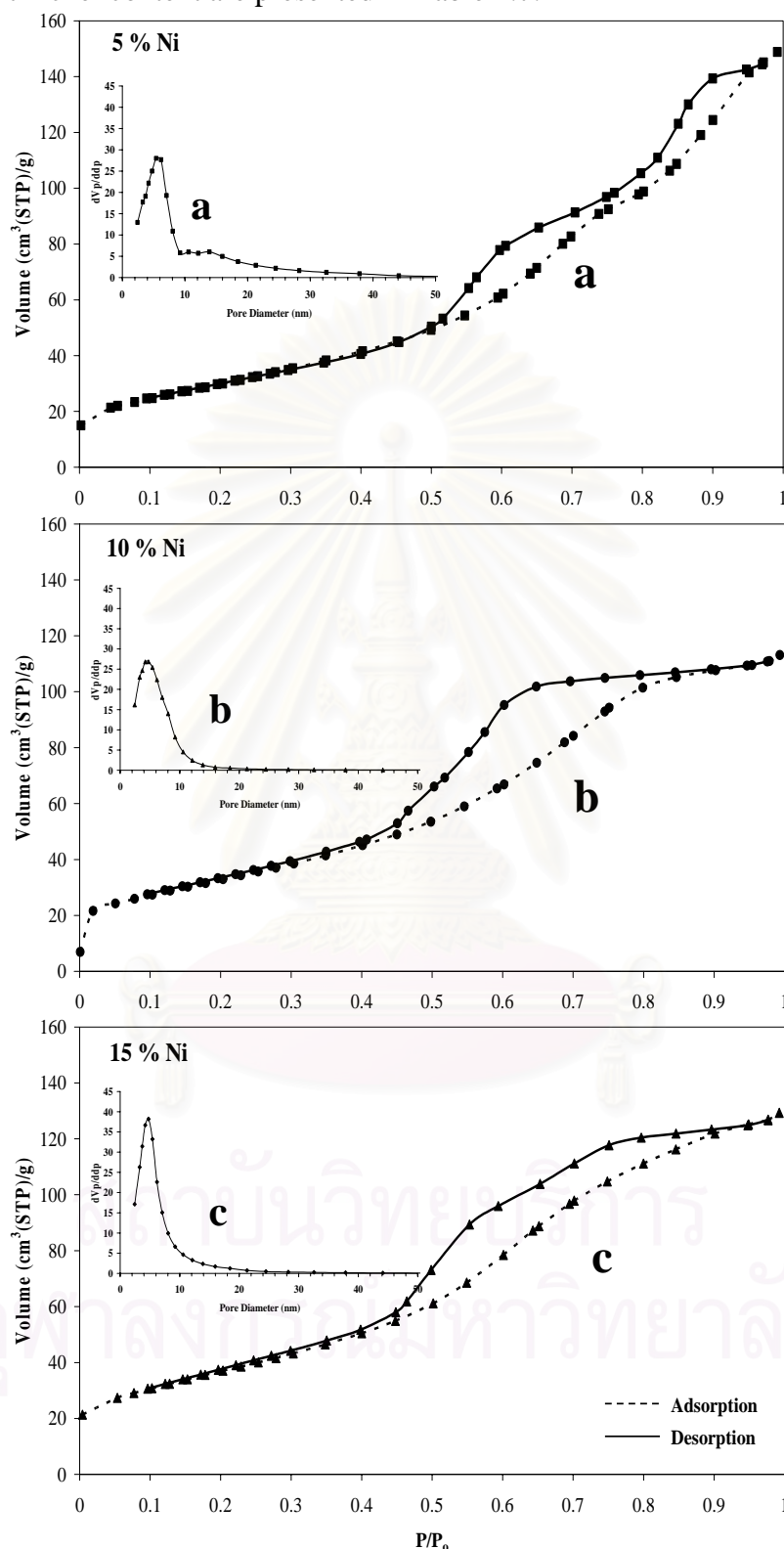


Figure 4.8 Nitrogen adsorption-desorption isotherms and pore size distributions of mixed metal oxides of Ni/Mg/Zr prepared by CP method with different nickel contents.

BET isotherms of the mixed metal oxides with different % wt Ni all match with type IV with hysteresis effect.

Table 4.7 Characteristics of mixed metal oxides of Ni/Mg/Zr prepared by CP method with different % wt Ni

% wt Ni	Surface area (m ² /g)	Pore volume (cm ³ /g)	Average pore size (nm)
5	111	0.23	8.2
10	121	0.20	5.7
15	136	0.17	5.9

From the data in Table 4.7, it was found that when increase % wt Ni, the surface area increases but the pore volume and pore size decrease. The reduction of pore volume might be attributed to an increase in the wall thickness [29]. The high surface area and the mesopore size is good characteristic of catalyst.

4.3 Citric acid precursor technique (CT)

4.3.1 Effect of calcination temperature

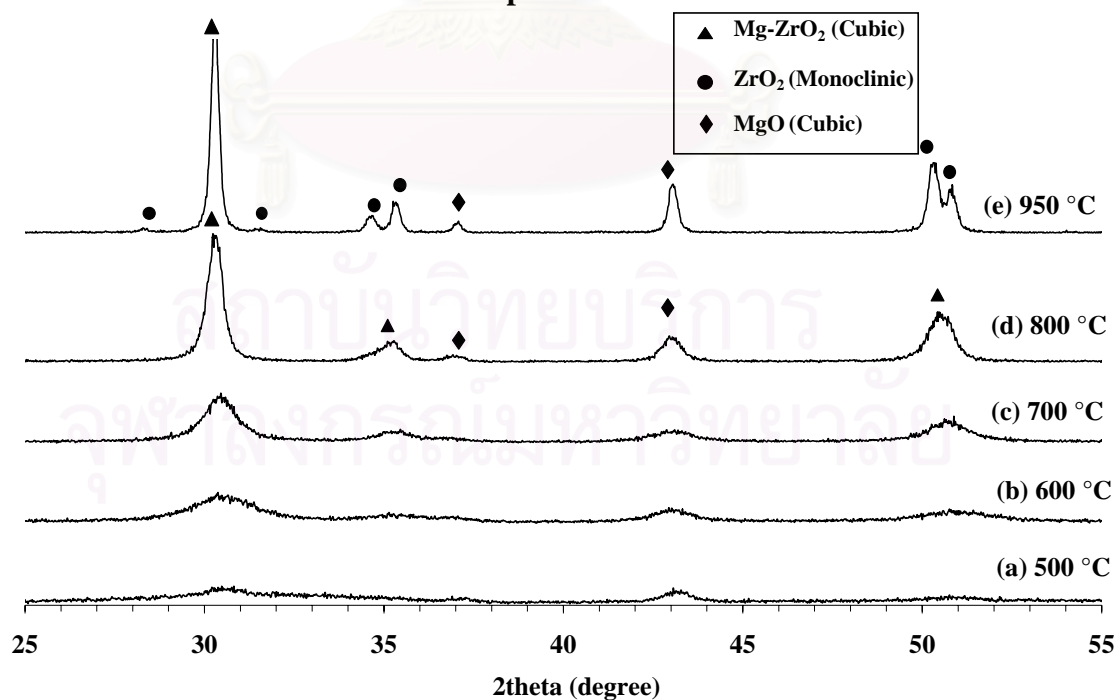


Figure 4.9 XRD diagrams of mixed metal oxides of Ni/Mg/Zr prepared by CT method at different calcination temperature (15%Ni, Mg/Zr molar ratio =1, time 6 h.).

From XRD, at calcination temperature around 700-800°C, only Mg-ZrO₂ phase was present ($2\theta = 30.6, 35.4, 50.9, 60.5, 63.5$). The phase change was observed when temperature was increased to 950°C. MgO was present.

The data of crystallite size and lattice parameter are listed in Table 4.8.

Table 4.8 Characteristics of mixed metal oxides of Ni/Mg/Zr prepared by CT method annealed at different calcinations temperature

Calcination temperature (°C)	Crystallite size (nm)	Phase	Lattice parameter of Mg-ZrO ₂ (Å)		
			a	b	c
500	20	Mg-ZrO ₂ cubic	5.09	5.09	5.09
600	14	Mg-ZrO ₂ cubic	5.09	5.09	5.09
700	11	Mg-ZrO ₂ cubic	5.09	5.09	5.09
800	17	Mg-ZrO ₂ cubic	5.09	5.09	5.09
950	35	Mg-ZrO ₂ cubic	5.09	5.09	5.09
	60	ZrO ₂ monoclinic	5.14	5.20	5.31

The Mg-ZrO₂ crystallites show cubic pattern with unit cell dimension of 5.09 Å. The ZrO₂ has unit cell dimension of 5.14 (a), 5.20 (b), 5.31 (c) Å.

From the result obtained, it showed that the optimum calcination temperature in the CT method is at 800°C as only Mg-ZrO₂ phase was detected.

4.3.2 Effect of calcination time

Mixed oxides of Ni/Mg/Zr, Mg/Zr molar ratio =1, 15% wt Ni were calcined at 800°C on different time. XRD patterns are shown in Figure 4.10

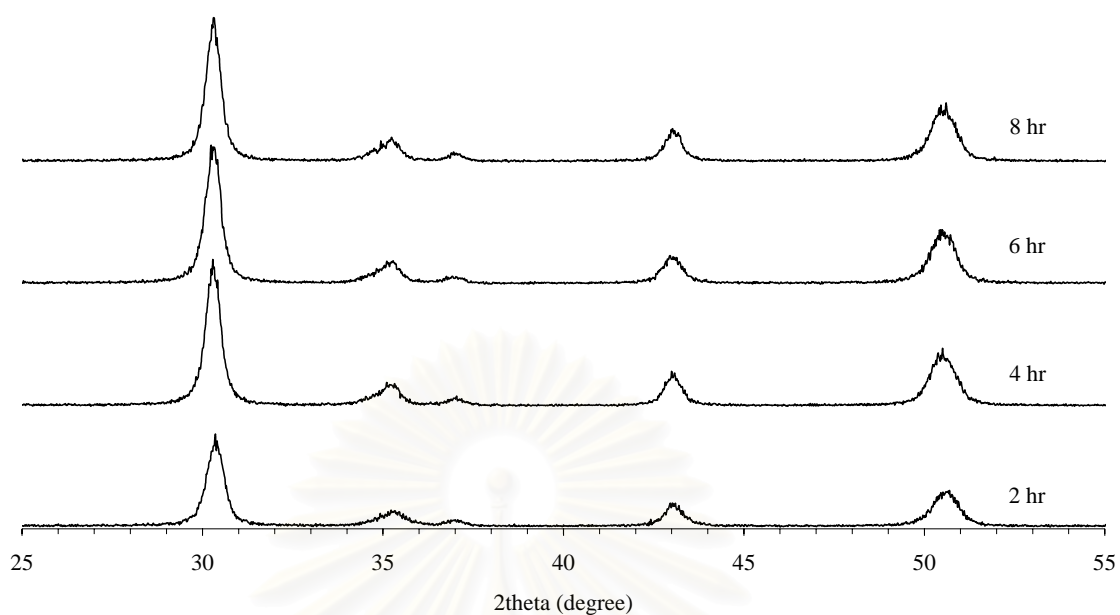


Figure 4.10 XRD diagrams of mixed metal oxides of Ni/Mg/Zr prepared by CT method annealed at different time (15%Ni, mole ratio Mg/Zr =1, temp. = 800°C).

As found in the CP method, in the CT method, the calcination time does not affect to the properties of the mixed oxides, except that % crystallinity increases with calcination time. Time of 4 h. is adequate to obtain high crystallinity, therefore, this is used in further experiments.

Table 4.9 Characteristics of mixed metal oxides of Ni/Mg/Zr prepared by CT method calcined at different time

Calcination time (h)	Relative crystallinity (%)	Crystallite size (nm)	Lattice parameter of Mg-ZrO ₂ (Å)
2	65	17	5.09
4	100	18	5.10
6	100	17	5.10
8	100	18	5.10

4.3.3 Effect of Mg/Zr molar ratio

XRD patterns of mixed metal oxides of Ni/Mg/Zr with different Mg/Zr molar ratio, 15% wt Ni at calcination temperature of 800°C and calcinations time = 4 h are shown in Figure 4.11. The relative crystallinity, crystalline size and lattice parameter are listed in Table 4.10.

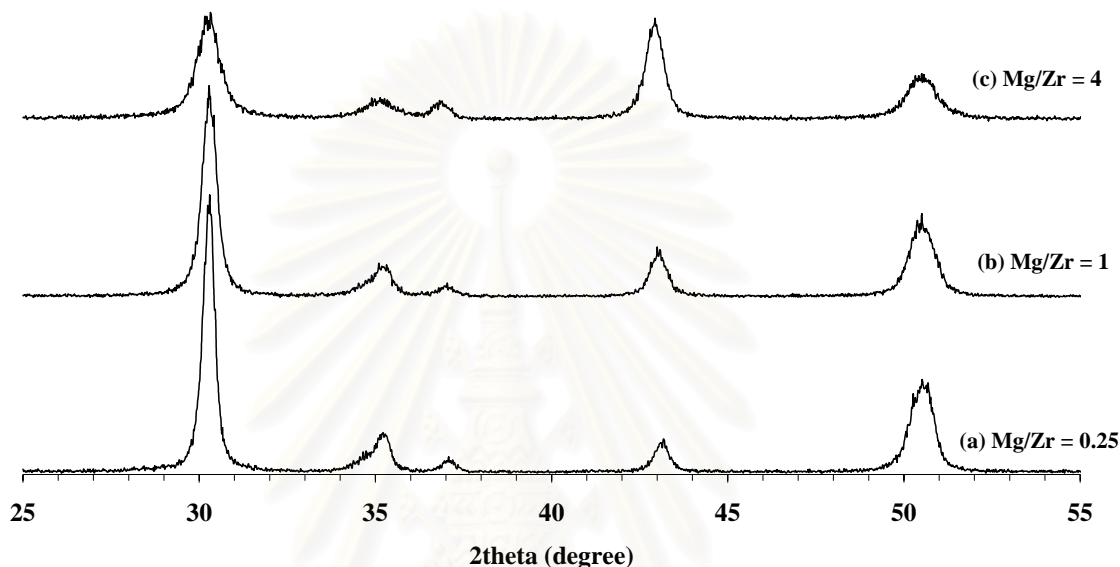


Figure 4.11 XRD diagrams of mixed metal oxides of Ni/Mg/Zr prepared by CT method with different Mg/Zr molar ratio (15% wt Ni, calcination temp = 800°C, calcination time = 4 h.).

When Mg/Zr molar ratio was increased (that is higher Mg content, the oxide has smaller crystallite size. In addition, lower %crystallinity of the oxide was resulted.

Table 4.10 Characteristics of mixed metal oxides of Ni/Mg/Zr with different Mg/Zr molar ratio

Mg/Zr Molar ratio	Relative crystallinity (%)	Crystallite size (nm)	Lattice parameter of Mg-ZrO ₂ (Å)
0.25	100	22	5.10
1	73	17	5.10
4	40	13	5.11

N_2 adsorption-desorption isotherm and pore size distributions of the mixed metal oxides with different Mg/Zr molar ratio are shown in Figures 4.12.

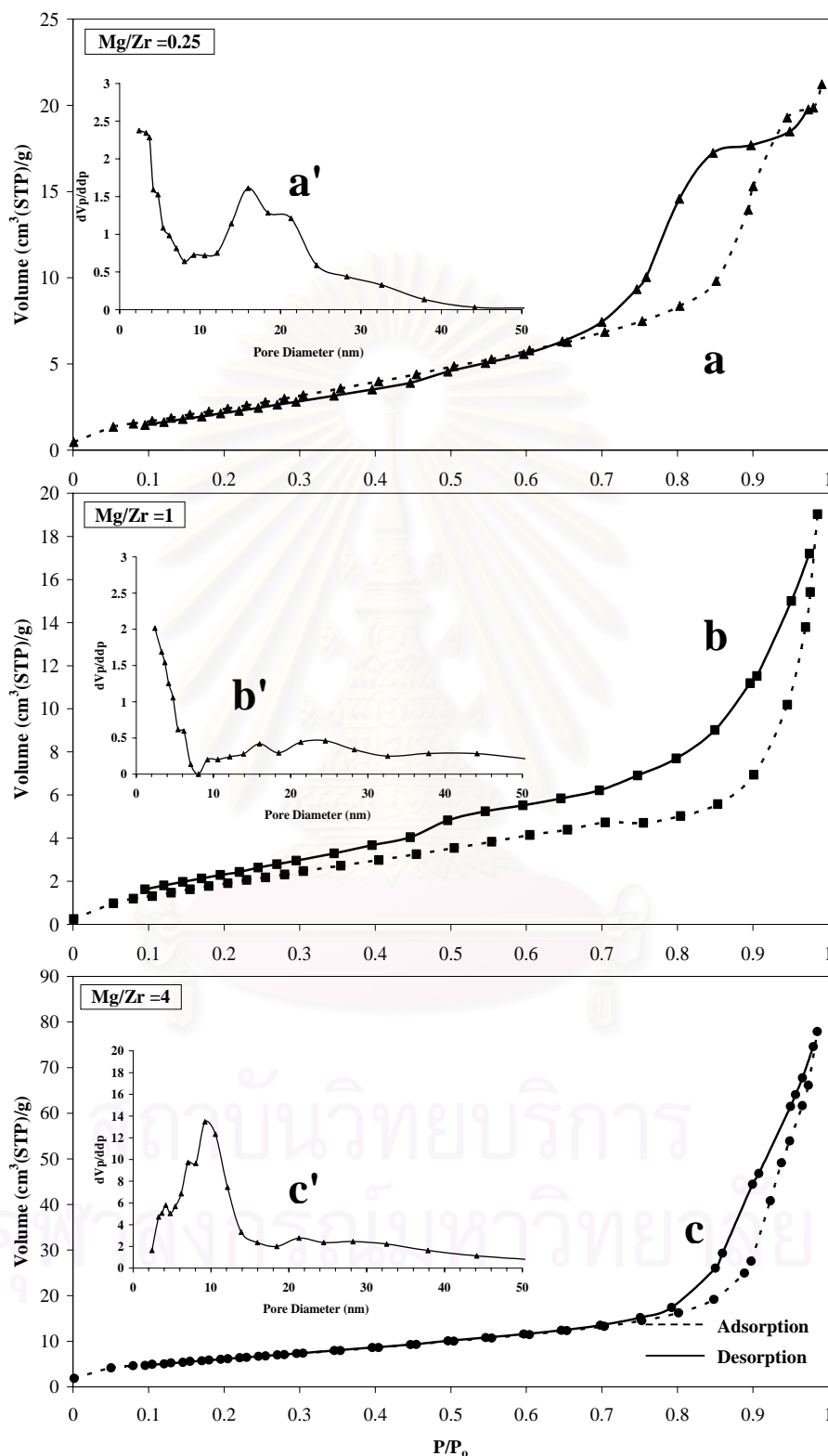


Figure 4.12 Nitrogen adsorption-desorption isotherms and pore size distributions of mixed metal oxides of Ni/Mg/Zr prepared by CT method with different Mg/Zr molar ratio

N_2 adsorption-desorption isotherms of mixed oxides with different molar ratio of Mg/Zr matched in type IV.

It is absorption and evaporation of gas occurred from condensation that evaporated on small pore size catalyst. The small pore size from hysteresis effect is long bar which different opened end.

The pore size distributions show that at Mg/Zr molar ratio = 0.25, there are two pore sizes: micropores and mesopores. The different pore sizes might be due to citric acid precursor which was burnt to carbon after calcination.

Table 4.11. Characteristics of mixed metal oxides of Ni/Mg/Zr prepared by CT method with different Mg/Zr molar ratio (calcined in air at 800°C for 4 h.).

Mg/Zr Molar ratio	Surface area (m ² /g)	Pore volume (cm ³ /g)	Average pore size (nm)
0.25	11	0.03	11.7
1	9	0.03	13.0
4	6	0.02	15.5

From the data it was found that the highest surface area of Mg/Zr was obtained at Mg/Zr molar ratio = 0.25. The pore size is in the range of mesopores.

4.3.4 Effect of citric acid content

Mixed metal oxides of Ni/Mg/Zr, Mg/Zr molar ratio = 0.25, with 15% wt Ni were calcined at 800°C, time 4h. In order to see whether amount of citric acid has any effect on the oxide surface area, citric acid/total cation molar ratio was varied. The results are shown in Figure. 4.13 and Table 4.12.

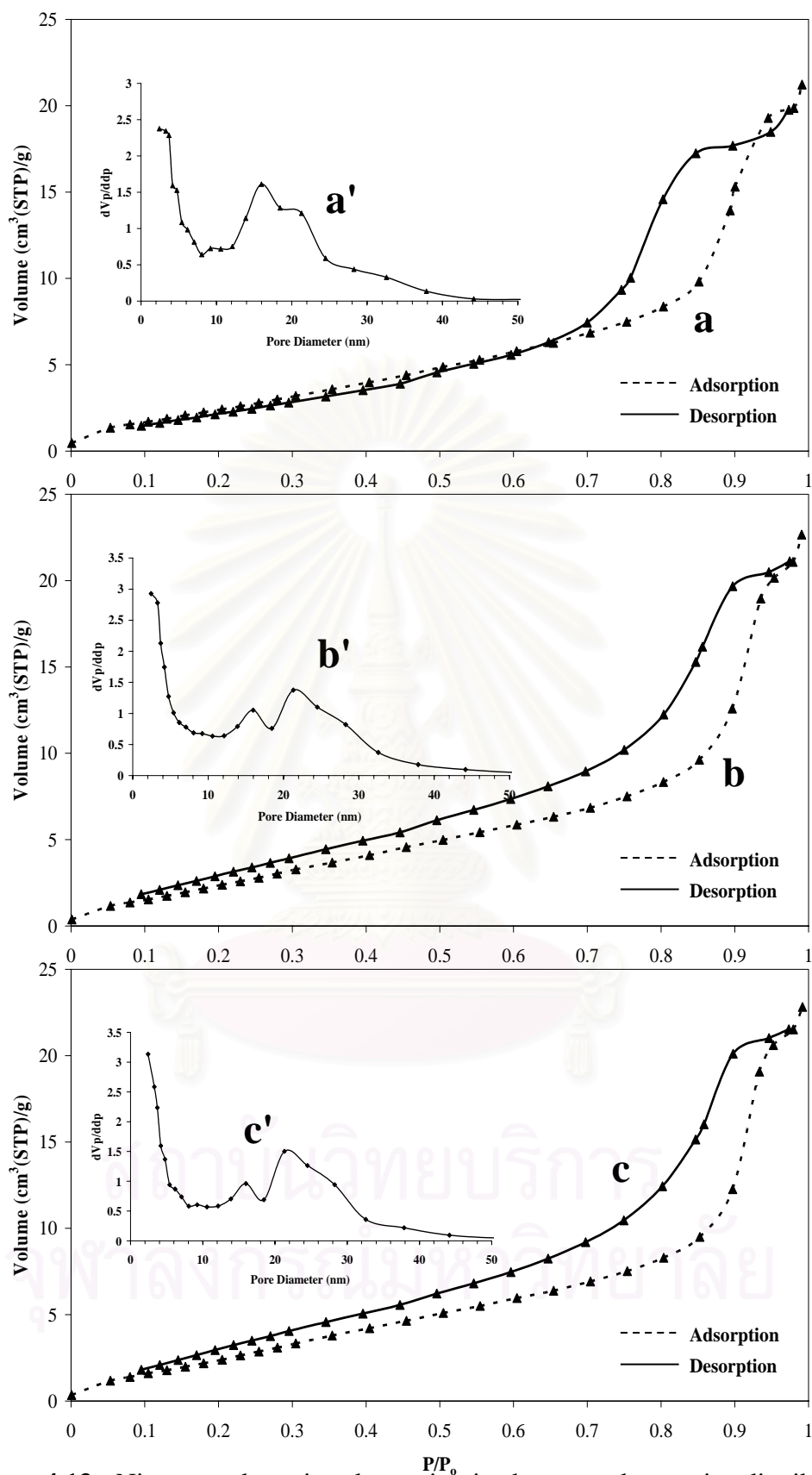


Figure 4.13 Nitrogen adsorption-desorption isotherms and pore size distributions of mixed metal oxides of Ni/Mg/Zr prepared by CT method with different citric acid content.

From Figure 4.13 a', b' and c', the samples are not homogeneous, two dominant pore sizes are observed.

Table 4.13 Characteristics of mixed metal oxides of Ni/Mg/Zr prepared by CT method with different citric acid content

Citric acid/Total cation Mole ratio	Surface area (m²/g)	Pore volume (cm³/g)	Average pore size (nm)
1.0	11	0.0326	11.7
1.5	12	0.0350	11.2
2.0	12	0.0349	11.2

Comparing to the CP method, surface area of the mixed oxides obtained from the CT method is quite lower than that from the CP method. The pore size lies in the mesoporous range, around 11 nm.

From the data, it was seen that different citric acid content does not affect the surface area, pore volume and pore size.

4.4 Modified citric acid precursor technique (MCT)

Modified citric acid precursor technique (MCT) is similar to the CT technique except that there are two steps for calcination. First, the pyrolysis was carried out under nitrogen at 800°C for one hour and followed by calcination step under air for three hours. Citric acid/total cation mole ratio is varied. Nitrogen adsorption-desorption isotherms are displayed in Figure 4.14. The surface area, pore volume and pore size are shown in Table 4.14.

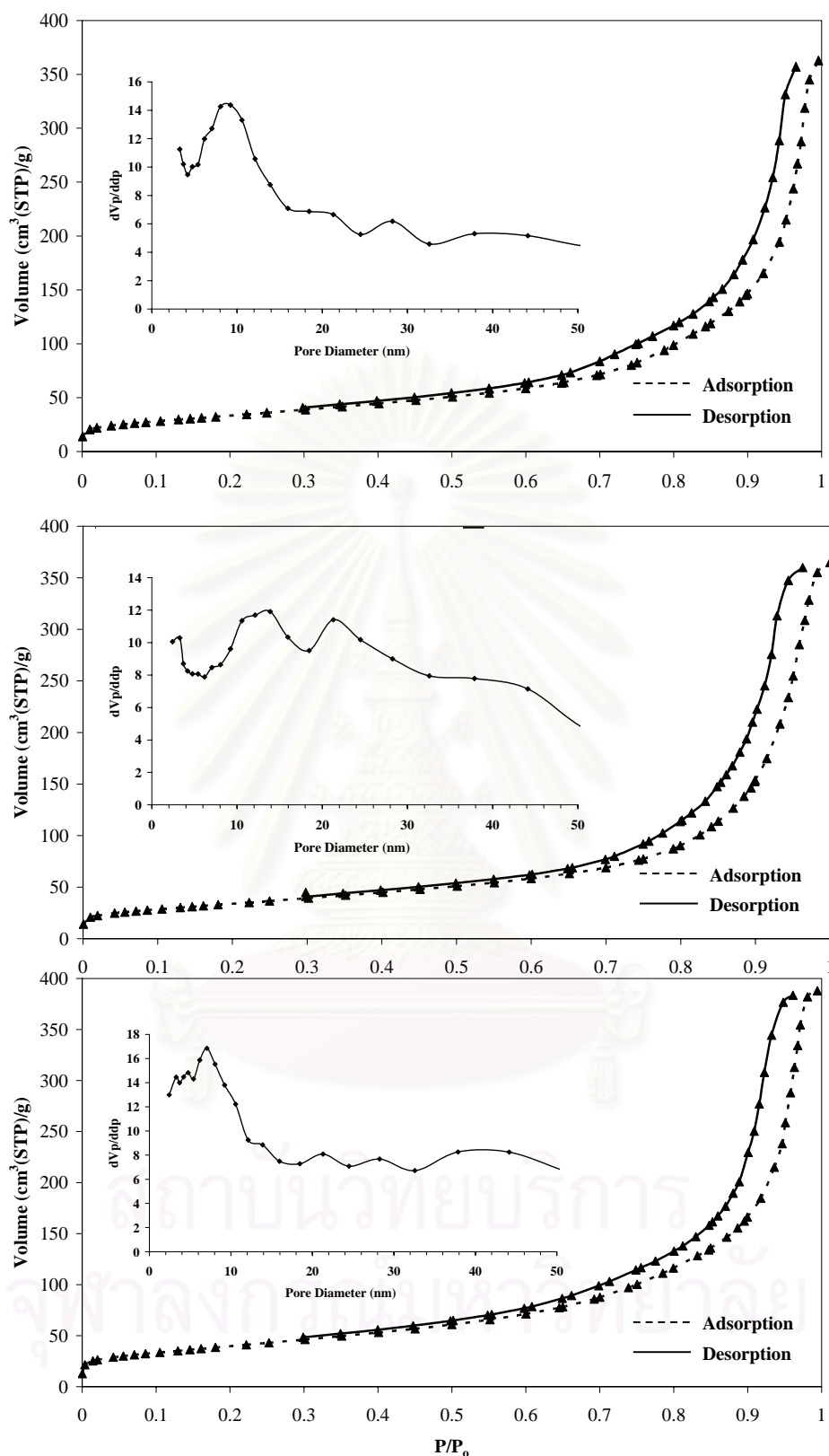


Figure 4.14 Nitrogen adsorption-desorption isotherms and pore size distributions of mixed metal oxides of Ni/Mg/Zr prepared by MCT method with different citric acid content

Their BET isotherms match with type IV with hysteresis effect.

Table 4.14 Characteristics of mixed metal oxides of Ni/Mg/Zr prepared by MCT method with different citric acid content

Citric acid/Total cation Molar ratio	Surface area (m ² /g)	Pore volume (cm ³ /g)	Average pore size (nm)
1.0	122	0.5497	18.0
1.5	124	0.5553	17.9
2.0	145	0.5968	16.4

The mixed metal oxides possess high surface area and have pore size in the mesoporous range, around 16.4–18.0 nm.

It was found that when citric acid content was increased, the surface areas and the pore volumes increase, but the pore sizes decrease. The high surface areas and the large pore volume are attributed to the carbon content in the oxide which was burnt out during pyrolysis, resulting in increasing porosity. [28] The formation of mixed oxides is as shown in Figure 4.15.

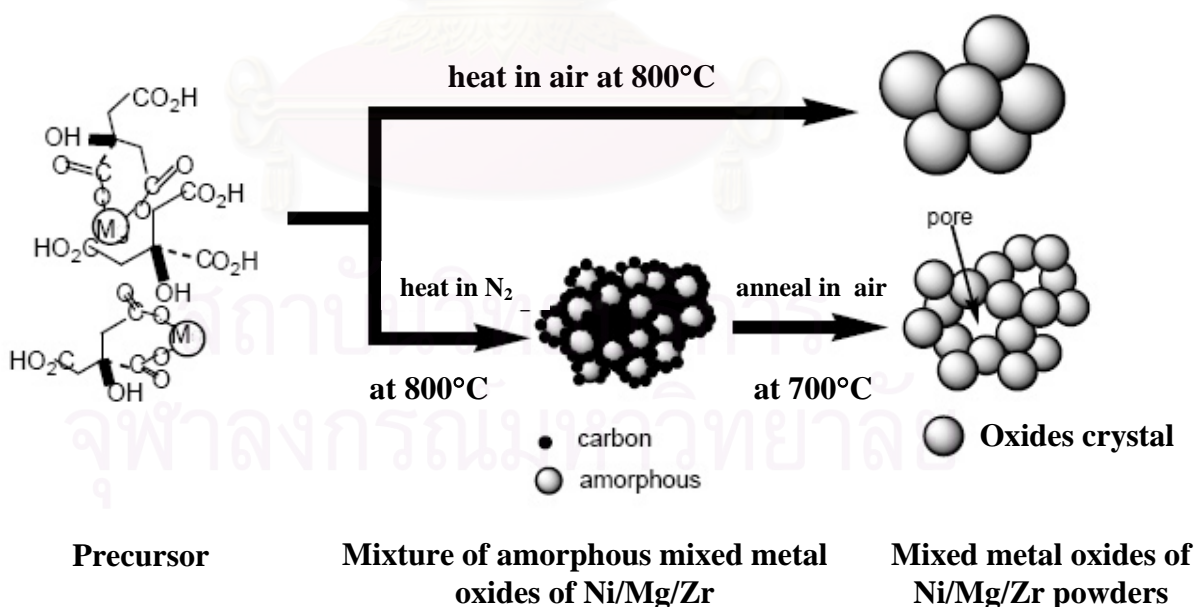


Figure 4.15 Schematic diagram of formation of mixed metal oxides from citric acid precursor.

Thermogravimetric analysis (TG)

In this work TGA was used to monitor the pyrolysis process. The TGA profile of mixed metal oxides of Ni/Mg/Zr prepared from the citric acid precursor method (CP) after the pyrolysis step was shown in Figure 4.16.

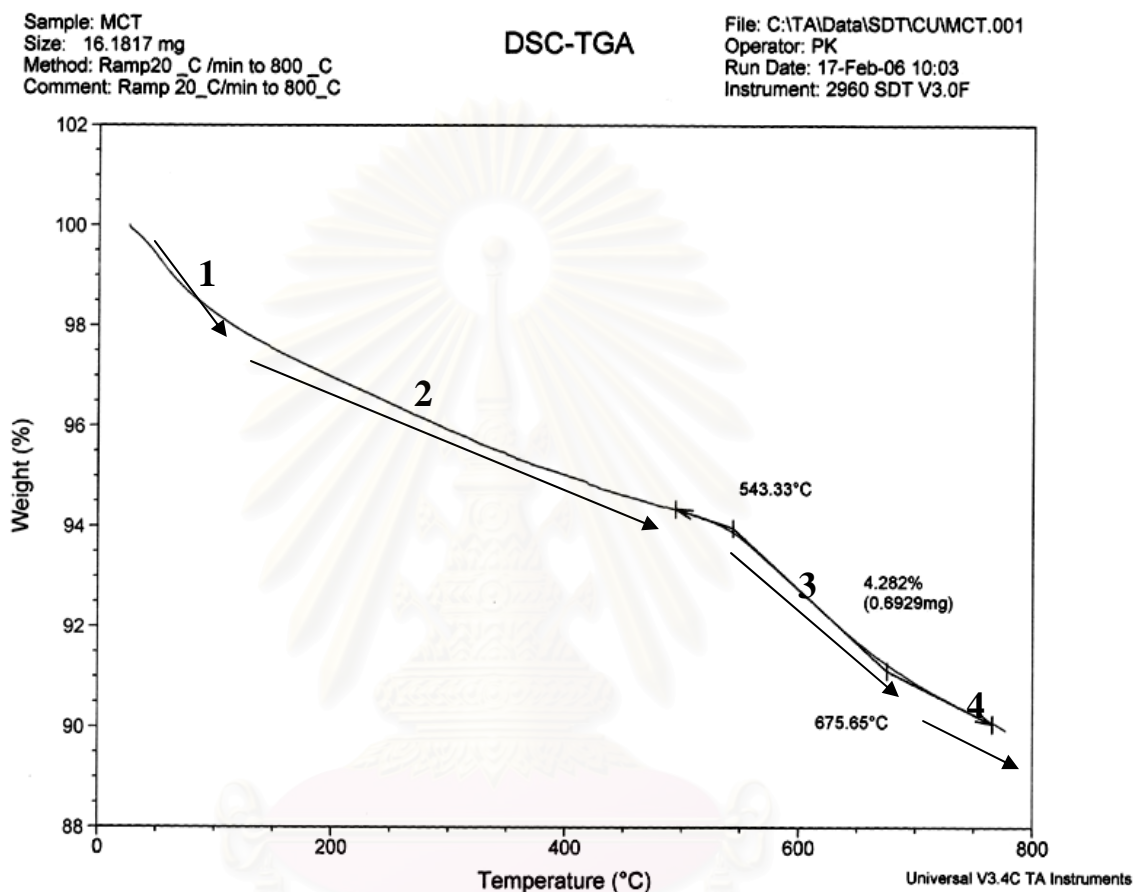


Figure 4.16 TGA profile of mixed metal oxides of Ni/Mg/Zr prepared by MCT method.

In the temperature range of room temperature (33°C) to 800°C, the TGA curves show four steps of weight loss.

The first one occurred up to 120°C which is due to dehydration of the powder precursor.

The second one, between 150 and 500°C, which is due to carbonization of the residual carbon or bond breaking of organic moieties in precursors together with the evolution of great amounts of gases such as CO₂ and H₂O.

The third and fourth weight losses (~4%) around 500-775°C are attributed to burnout of the remaining organic species in the powder precursor.

4.5 Modified citric acid/ethylene glycol precursor technique (MCTE)

In this method, suitable conditions found from the CT method are used. Ethylene glycol is added as another precursor. Two steps of calcination were carried out, first under nitrogen at 800°C for 1 h., followed by under air for 3 h. Ethylene glycol content was varied. Nitrogen adsorption-desorption isotherms are displayed in Figure 4.17. The surface area, pore volume and average pore size are shown in Table 4.15.

BET isotherms match with type II with hysteresis effect. When comparing between the mixed metal oxides prepared by the MCT and the MCTE method, it can be seen that they are different. MCTE gives oxide with type II pattern, which means it has both physisorption and chemisorption.

Table 4.15 Characteristics of mixed metal oxides of Ni/Mg/Zr prepared by MCTE method with different ethylene glycol content (citric acid/total cation molar ratio = 2)

Citric acid/ ethylene glycol molar ratio	Surface area (m ² /g)	Pore volume (cm ³ /g)	Average pore size (nm)
1.0	120	0.5438	18.1
1.5	141	0.5292	15.0
2.0	144	0.5021	12.1

The mixed metal oxides prepared by the MCTE have high surface area and pore size is in the mesoporous range, around 12.1–18.1 nm.

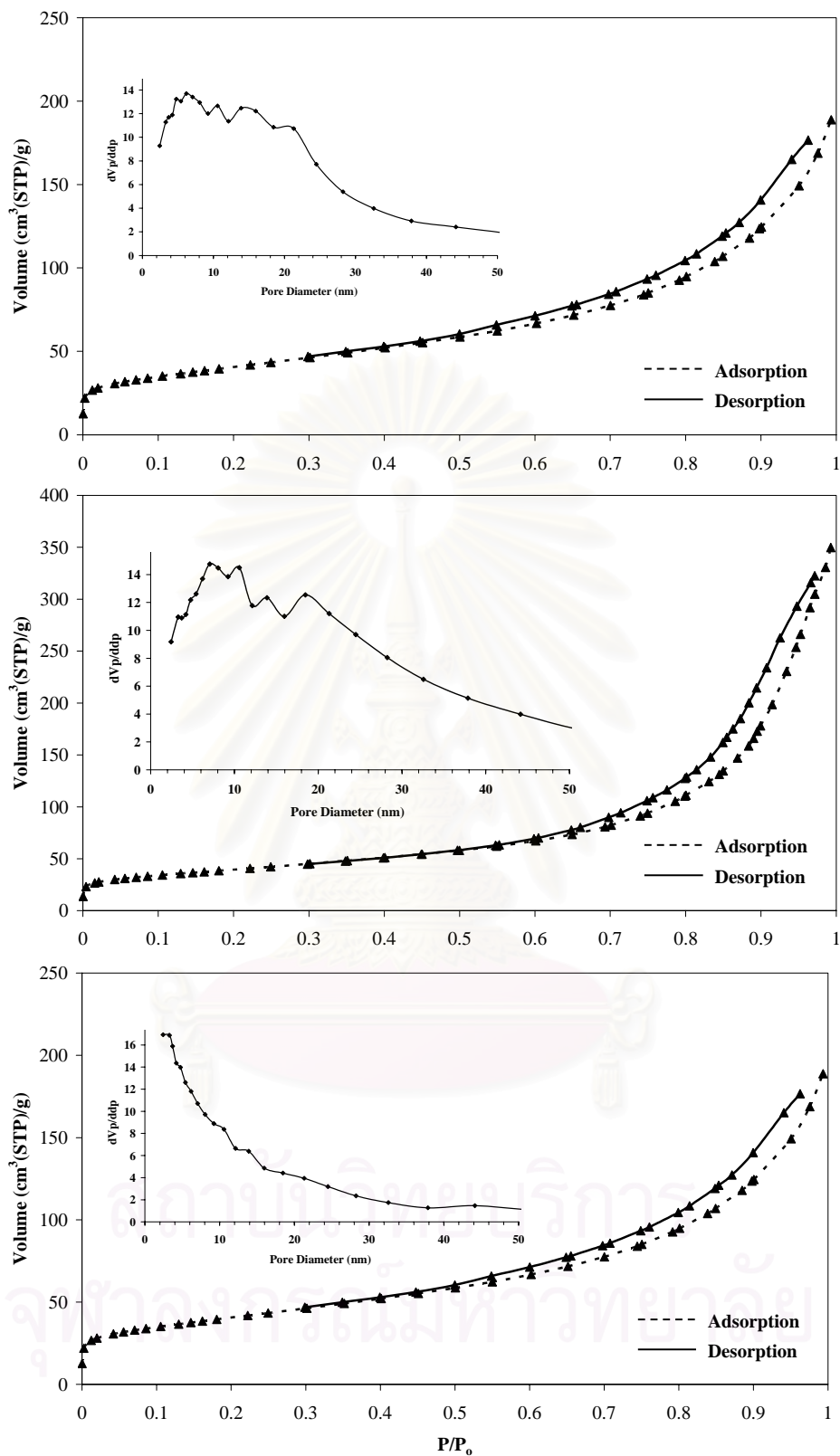


Figure 4.17. Nitrogen adsorption-desorption isotherms and pore size distributions of mixed metal oxides of Ni/Mg/Zr prepared by MCTE method with different ethylene glycol content

In summary, it can be seen that the optimum conditions for each method are different and they are tabulated in Table 4.13.

Table 4.16 Optimum conditions in each method

Method	Temperature (°C)	Time (h)	Mg/Zr Molar ratio	Citric acid/cation Molar ratio	Citric acid/ethylene glycol Molar ratio
CP	600	4	0.25	-	-
CT	800	4	0.25	1.5-2.0	-
MCT	800	4	0.25	2.0	-
MCTE	800	4	0.25	2.0	2.0

4.6 Characterization

4.6.1 Fourier-transform infrared spectroscopy (FT-IR)

FTIR spectra of the mixed metal oxides of Ni/Mg/Zr prepared by different methods are taken and summarized in Table 4.17.

Table 4.17. FTIR spectra of mixed metal oxides of Ni/Mg/Zr prepared by different methods

Wave number (cm ⁻¹)				Assingment
CP	CT	MCT	MCTE	
3,388	3,450	3,679	3,456	OH- stretching
1,384	1,397	1,400	1,396	OH- bending
-	1,530	1,571	1,567	CO ₃
430	449	490	420	Ni-O stretching

FTIR spectra of the mixed metal oxides of Ni/Mg/Zr all show a broad absorption at about 3388 cm⁻¹, which is assigned to OH of water from moisture. The

absorption bands around 1571–1384 cm^{-1} indicates the existence of CO_3^{2-} which comes from the metal precursor used. Bands present around 440 cm^{-1} are from the Ni-O stretching [30].

4.6.2 Energy Dispersive X-ray Analysis (EDX)

EDX analyses for the atomic of elements composition on oxide surface are summarized in Table 4.18.

Table 4.18 EDX data of the mixed metal oxides prepared by different methods

	% Atomic			Mg/Zr Molar ratio
	Ni	Mg	Zr	
Actual	17.05	16.65	66.30	0.25
CP	19.01	17.87	63.12	0.28
CT	15.87	19.92	64.21	0.31
MCT	21.19	17.93	60.89	0.29
MCTE	18.80	18.87	62.34	0.30

By using EDX technique, %atomic of each element on oxide surface can be detected quantitatively. The results showed that the oxides prepared with CT method had lower %Ni than those prepared with other methods. The MCT method gave highest %Ni. When compared with the actual %Ni loaded, it seems that %Ni on the oxide surface is higher, this might reveal the accumulation of Ni on the surface. The similar result was obtained for %Mg on the oxide surface. This can be explained by the high amount of Mg loaded. It was reported that high amount of Mg is appropriate for the good catalyst, as it can decrease coke deposit [31].

4.6.3 Scanning electron microscopy (SEM)

The SEM micrographs of the mixed metal oxides of Ni/Mg/Zr prepared by 4 methods are displayed in Figure 4.18.

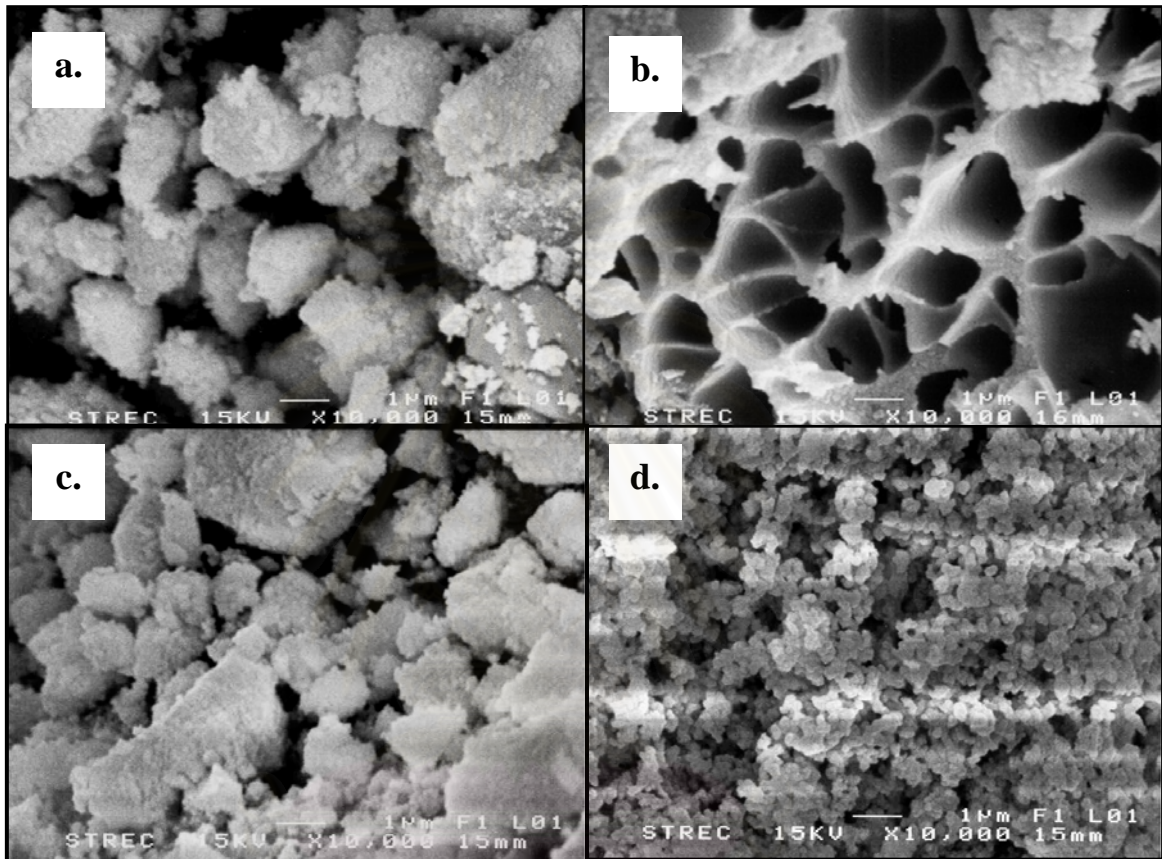


Figure 4.18 The SEM micrographs of the mixed metal oxides prepared by different methods

a. co-precipitation (CP)

b. citric acid precursor technique (CT)

c. modified citric acid precursor technique (MCT)

d. modified citric acid and ethylene glycol precursor technique (MCTE)

Comparison of the morphology between different preparation methods, it was shown that in the CP, MCT and MCTE methods, the oxide particle size has a spherical shape and homogeneous while in the CT method, after calcination at 800°C for 4 h. and adding citric acid, the morphology is inflated and cheese-like. It should be noted that the oxide particle sizes decreased in the order of CP > MCT > MCTE.

One point should be mentioned from the results obtained is that the oxides from the MCTE method have the smallest particle size ($0.2 \mu\text{m}$) but the pore volume and pore size are only a little smaller than from the MCT method. This might be due to the difference in the preparation conditions.

The occurrence of high surface areas can be attributed to the preparation method. While smaller particle sizes ($0.2 \mu\text{m}$) with a spherical-like morphology were observed for the catalyst obtained from MCTE method. The pore volume is $0.5021\text{cm}^3/\text{g}$, a little less than MCT method. However, the average pore size is less (12.1nm) than MCT method (16.4nm).

4.6.3 Transmission electron microscopy (TEM)

The TEM micrographs of the mixed metal oxides prepared by different methods are displayed in Figure 4.19.

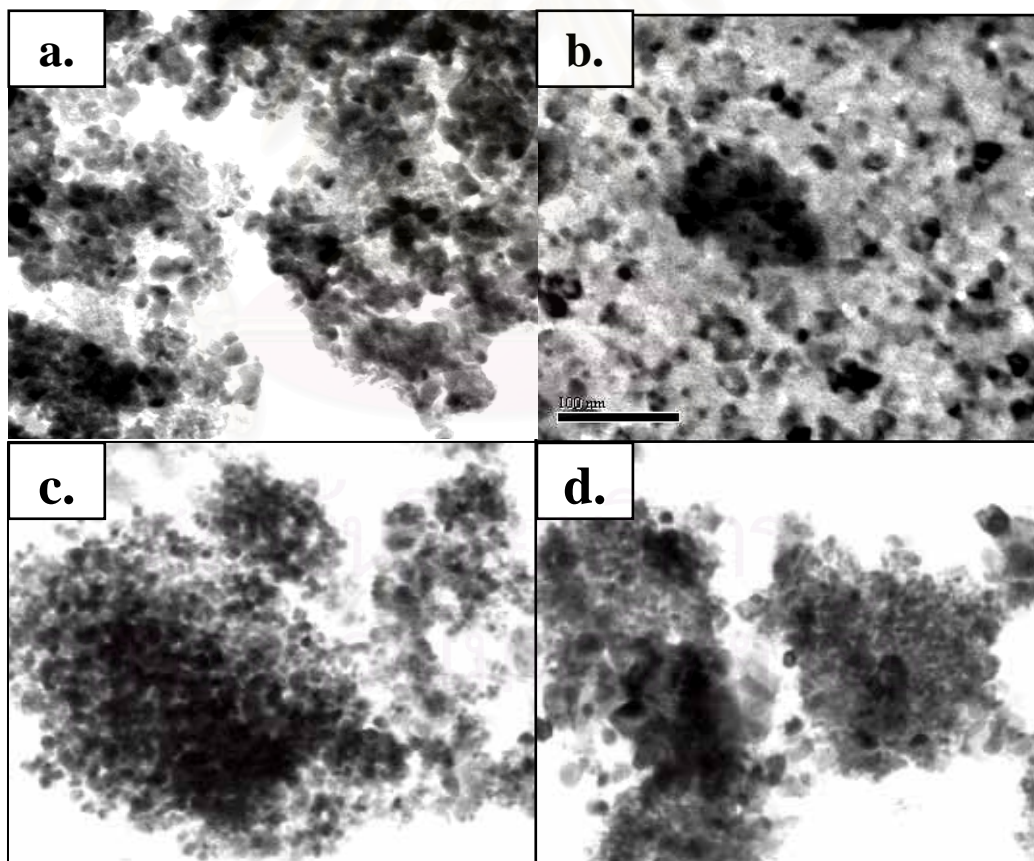


Figure 4.19 The TEM micrographs of the mixed metal oxides prepared by different methods. a. CP, b. CT, c. MCT and d. MCTE.

TEM technique helps to reveal the metal particle size. It was seen that bigger Ni particles (more than 20 nm) were detected in CP method (Figure 4.20b). While a large portion of smaller Ni particles ca. 5-10 nm were detected in the CP, MCT and MCTE methods (Figures 4.20 a, c and d).

From the image there are many uniform black dots on the background of the agglomerations, indicating homogenous dispersion of the Ni particles.

In summary, the characteristics of the mixed metal oxides prepared by different methods are shown in Table 4.19.

Table 4.19 Characteristics of the mixed metal oxides prepared by different methods

Method	Crystallite size (nm)	Surface area (m ² /g)	Pore volume (cm ³ /g)	Average pore size (nm)
CP	12	136	0.1993	5.9
CT	22	12	0.0349	11.2
MCT	18	145	0.5968	16.4
MCTE	20	144	0.5021	12.1

The different preparation methods lead to oxides with different characteristics. Each characteristic can be stated as follows:

Order of crystallite size MCTE > CT > MCT > CP

Order of surface area MCTE ~ MCT > CP > CT

Order of pore volume MCT > MCTE > CP > CT

Order of pore size MCT > MCTE ~ CT > CP

The high surface area mixed metal oxides obtained from this work are comparable to those reported. [30, 31, 32]

4.7 Surface properties of Sn doped the mixed metal oxides catalyst.

In reforming of methane with metal oxide catalyst, addition of Sn was reported to improve the dispersion of Ni particles and the stability of the catalysts, for example, PtSn catalyst [39] and SnNi catalyst [40, 41]. Therefore, in this work, the obtained mixed metal oxides of Ni/Mg/Zr has also added Sn and the resulting material was characterized by TEM. The TEM images are shown in Figure 4.20.

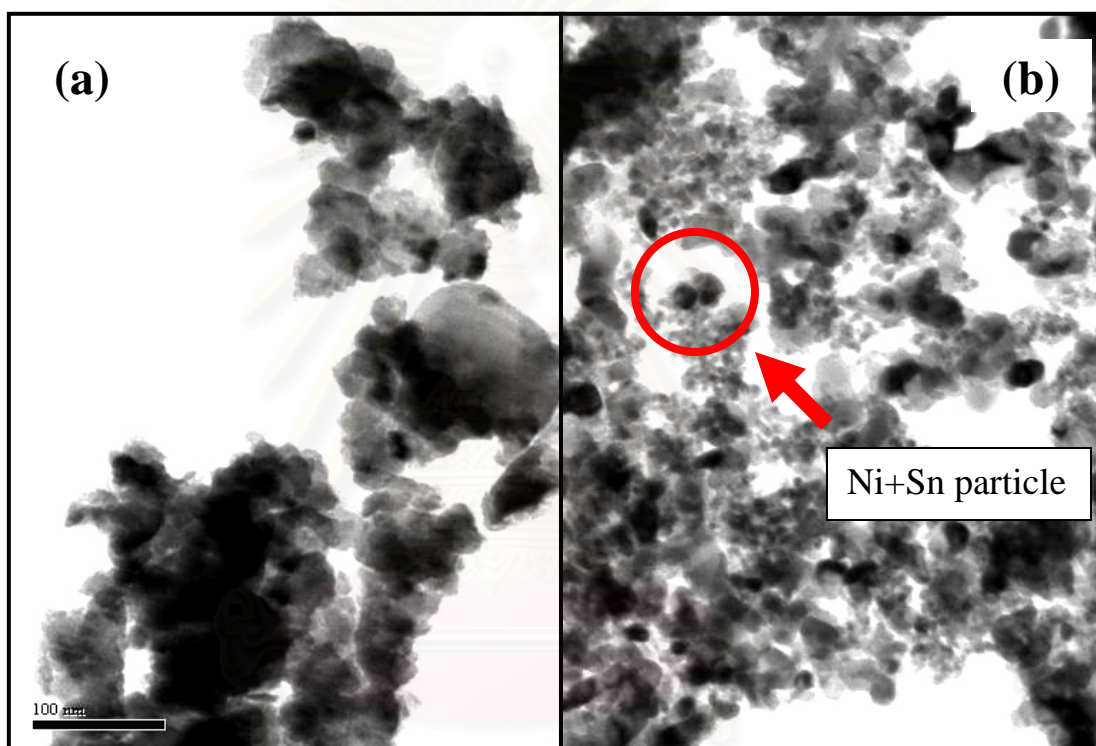


Figure 4.20 The TEM micrographs of mixed metal oxides of Ni/Mg/Zr prepared by MCT (15%wt Ni, Mg/Zr molar ratio = 0.25, calcination temperature = 800 °C, calcinations time = 4 h, citric acid/cation molar ratio =2) (a) No Sn doped (B) Sn (0.02 %mole) doped.

Smaller Ni particles (more than 10 nm) were seen in the mixed metal oxide which was doped with Sn. This result suggested that Sn can improve the dispersion of Ni particles. It was proposed that Sn retarded the sintering of Ni. [41]

CHAPTER V

CONCLUSION AND SUGGESTIONS

This research work is to prepare mixed metal oxides of Ni/Mg/Zr which can be used as catalyst in suitable reactions. The oxides from co-precipitation (CP), citric acid precursor technique (CT), modified citric acid precursor technique (MCT), modified citric acid/ethylene glycol precursor technique (MCTE) were characterized by X-ray Diffraction (XRD), Transmission Electron Microscopy (TEM), Scanning Electron Microscopy (SEM), Energy Dispersive X-ray Analysis (EDX), Fourier Transform Infrared spectroscopy (FTIR), Thermogravimetric Analysis (TGA) and Brunauer-Emmet-Teller (BET).

In the CP method, calcination was performed at lower temperature (600°C). This method yields oxides with high surface area of 136 m²/g but low pore size. By adding citric acid as a modifying agent in the CT method and one calcination, the oxides show very low surface area. Nevertheless, when performing two calcinations (in the MCT method), the oxides have high surface area (145 m²/g) and large pore size. Further modification with both citric acid and ethylene glycol (the MCTE method) yields oxides with high surface area (144 m²/g). In summary, the mixed metal oxides from the preparation methods attempted in this work was shown to possess the following characteristics:

- high surface area
- nanocrystalline
- nanoporous
- good metal dispersion
- good pore size distribution

Suggestion

From the results in this work, further work that should be continued is to utilize these prepared mixed metal oxides of Ni/Mg/Zr in reforming of methane.

References

1. Trimm, D.L. The formation and removal of coke from nickel catalyst. Catal. Rev. Sci. Eng. 16 (1977) : 155-189.
2. Rostrup-Nielsen, J.R. and Anderson M. Catalytic Transformation of greenhouse gases in a membrane reactor. Catalysis Science and Technology. 5 (1984) : 1-117.
3. Hickman, D.A. and Schmidt, L.D. Production of syngas by direct catalytic oxidation of methane. Science. 259 (1993) : 343-346.
4. Ruckenstein, E. and Hu, Y.H. The effect of precursor and preparation conditions of MgO on the CO₂ reforming of CH₄ over NiO/MgO catalysts. Applied Catalysis A: General. 154 (1997) : 185-205.
5. Choudhary, V.R.; Rajput, A.M. and Prabhakar, B. NiO/CaO-catalysed formation of syngas by coupled exothermic oxidative conversion and endothermic CO₂ and steam reforming of methane. Angew. Chem. Int. Ed. Engl. 33 (1994) : 2104 - 2106.
6. Ashcroft, A.T.; Cheetham, A.K.; Green, M.L.H. and Vernon, P.D.F. Partial oxidation of methane to synthesis gas using carbon dioxide. Nature. 352 (1991) : 225-226.
7. Rostrup-Nielsen, J.R. CO reforming of methane over LaNiO as starting material. J. Catal. 33 (1974) : 184-193.
8. Zhang, Y. and Smith, K. J., CH₄ decomposition on Co catalysts: effect of temperature, dispersion, and the presence of H₂ or CO in the feed. Catal. Today. 77 (2002) : 257-268.
9. Tomishige, K., Fujimoto, K. Ultra-stable Ni catalysts for methane reforming by carbon dioxide. J. Chem. Soc., Chem. Commu. 2 (1995) : 3-15.
10. Alvarado, E.; Tores-Martinez, L.M.; Fuentes, A.F.; Quintana, P. Synthesis molecular structure and reactivity of a calix arene monomethyl ether supported nitridomolybdenum complex. Polyhedron. 19 (2000) : 2345-2350.

11. Alonso, G.; Espino, J.; Berhault, G.; Alvarez, L. and Rico, L. Activation of tetraalkylammonium thiotungstates for the preparation of Ni-promoted WS₂ catalysts. Applied Catalysis A:general. 266 (2004) : 29-40.
12. Omata, K.; Nukui, N.; Hottai, T. and Yamada, M. Cobalt–magnesia catalyst by oxalate co-precipitation method for dry reforming of methane under pressure. Catal. Communications. 5 (2004) : 771-777.
13. Li, X.; Chan, J.S.; Tian, M. and Park, S. E. CO₂ reforming of methane over modified Ni/ZrO₂ catalysts. Appl. Organometal. Chem. 15 (2001) : 109 - 112.
14. Roh, H.-S.; Jun, K.-W.; Baek, S.-C. and Park, S.-E. A highly active and stable catalyst for carbon dioxide reforming of methane: Ni/Ce-ZrO₂/γ-Al₂O₃. Catal. Lett. 81(3-4) (2002) : 147-151.
15. Pejova, B.; Kocareva, T.; Najdoski, M. and Grozdanov, I. Solution growth route to nanocrystalline nickel oxide thin films. Appl. Surf. Sci. 165 (2000) : 271–278.
16. Biju, V. and Abdul K. M. AC conductivity of nanostructured nickel oxide. Spectrochim. Acta, Part A: Mol. Biomol. Spectrosc. 59 (2003) : 121– 124.
17. Sing, K.S.W.; Everett, D.H.; Haul, R.A.W.; Moscou, L.; Pietotti, R.A.; Rouquerol, J. and Siemienieska, T. Reporting physisorption data for gas/solid systems with special reference to the determination of surface area and porosity. Surface Pure Appl. Chem. 57 (1985) : 603-619.
18. Parmentier, J.; Richard-Plouet, M. and Vilminot, S. Sol-gel mono- and poly-component nanosized powders in the Al₂O₃-TiO₂-SiO₂-MgO system. Mater. Res. Bull. 33 (1998) : 1717-1724.
19. Rostrup-Nielsen, J.R. and Hansen, J.-H.B. First-principles study of C adsorption, O adsorption, and CO dissociation on flat and stepped Ni surfaces. J. Catal. 44 (1993) : 38-42.
20. Bradford, M.C.J. and Vannice, M.A. CO₂ Reforming of CH₄ over supported Ru catalysts. Journal of Catalysis. 183 (1999) : 69-75.
21. Rostrup-Nielsen, J.R. A highly effective catalyst for CO₂ reforming of methane: Ni/Ce-ZrO₂/γ-Al₂O₃. Stud. Surf. Sci. Catal. 36 (1998) : 73-76.

22. Barrett, E.P.; Joyner, L.G. and Halenda, P.P. The determination of pore volume and area distributions in porous substances. I. Computations from nitrogen isotherms. J. Amer. Chem. Soc. 73 (1951) : 373-380.
23. Makovicka, C.; Gärtner, G.; Hardt, A.; Hermann, W. and Wiechert, D.U. Impregnated cathode surface investigations by SFM/STM and SEM/EDX. Applied Surface Science. 111 (1997) : 70-75.
24. Ormstad, H.; Namork, E.; Gaarder, P.I. and Johansen, B. V. Scanning electron microscopy of immunogold labeled cat allergens (Fel d 1) on the surface of airborne house dust particles. Journal of Immunological Methods. 187 (1995) : 245-251.
25. Bals, S.; Kabius, B.; Haider, M.; Radmilovic, V. and Kisielowski, C. Annular dark field imaging in a TEM. Solid State Communications. 130 (2004) : 675-680.
22. Hegarty, M.E.S.; O'Connor, A.M. and Ross, J.R.H. Combination of carbon dioxide reforming and partial oxidation of methane over supported platinum catalysts. Catal. Today. 42 (1998) : 225-232.
23. Junmei, W and Enrique I. Structural requirements and reaction pathways in methane activation and chemical conversion catalyzed by rhodium. Journal of Catalysis. 225 (2004) : 116-127.
24. Stagg, S.M. E.; Romeo, C.; Padro, D. and Resasco. On the preparation of high surface-area nano-zirconia by reflux-digestion of hydrous zirconia Gel in Basic Solution. J. Catal. 178 (1998) : 137-145.
25. Cinibulk, M.K. Synthesis of yttrium aluminum garnet from a mixed-metal citrate precursor. J. Am. Ceram. Soc. 83 (2000) : 1276-1278.
26. Ruckenstein, E. and Hu, Y.H. The effect of precursor and preparation conditions of MgO on the CO₂ reforming of CH₄ over NiO/MgO catalysts. Applied Catalysis A: General. 154 (1997) : 185-205.
27. Frusteri, F; Arena, F.; Calogero, G.; Torre, T. and Parmaliana, A. Potassium-enhanced stability of Ni/MgO catalysts in the dry-reforming of methane. Catalysis Communications. 2 (2001) : 49-56.

28. Potdar, H.S.; Roh, H.S.; Jun, K.W. and Liu, Z.W. Carbon dioxide reforming of methane over co-precipitated Ni-Ce-ZrO₂ catalysts, Catalysis Letters. 84 (2002) : 95-106.
29. Valentini, A.; Carreno, N.L.V.; Probst, L.F.D. Leite, E.R. and Longo, E. Synthesis of Ni nanoparticles in microporous and mesoporous Al and Mg oxides, Microporous and Mesoporous Materials. 68 (2004) : 151-157.
30. Guo, J.; Lou, H.; Zhao, H.; Wang, X. and Zheng, X. Novel synthesis of high surface area MgAl₂O₄ spinel as catalyst support, Materials Letters. 58 (2004) : 1920-1923.
31. Bouarab, R.; Akdimb, O.; Auroux, A., Cherifi, O. and Mirodatos, C. Effect of MgO additive on catalytic properties of Co/SiO₂ in the dry reforming of methane. Applied Catalysis A: General. 264 (2004) : 161–168.
32. Song, C. and Pan, W. Tri-reforming of methane: a novel concept for catalytic production of industrially useful synthesis gas with desired H₂/CO ratio, Catalysis Today. 98 (2004) : 257-268.
33. Guo, J.; Lou, H.; Zhao, H.; Chai, D. and Zheng, X. Dry reforming of methane over nickel catalysts supported on magnesium aluminate spinels. Applied Catalysis A: General. 273 (2004) : 75–82.
34. Chen, L.; Sun, X.; Liu, Y. and Li, Y. Preparation and characterization of porous MgO and NiO/MgO nanocomposites, Appl. Catal. 256 (2004) : 123-128.
35. Montemayor, S.M.; Garcia-Cerda, L.A. and Torres-Lubian, J.R. Preparation and characterization of cobalt ferrite by the polymerized complex method, Materials Letters. 59 (2005) : 1056-1060.
36. Roh, H.S.; Potdar, H.S. and Jun, K.W. Carbon dioxide reforming of methane over co-precipitated Ni-CeO₂, Ni-ZrO₂ and Ni-Ce-ZrO₂ catalysts. Catalysis Today. 93-95 (2004) : 39-44.
37. Hou, Z.; Yokotab, O.; Tanakab, T. and Yashimab, T. Surface properties of a coke-free Sn doped nickel catalyst for the CO₂ reforming of methane. Applied Surface Science. 233 (2004) : 58–68.

38. Mariappan, C.R.; Galven, C.; Crosnier-Lopez, M.P.; Berre, F.L. and. Bohnke, O. Synthesis of nanostructured $\text{LiTi}_2(\text{PO}_4)_3$ powder by Pechini-type polymerizable complex method. Journal of Solid State Chemistry. 179 (2006) : 476-482.
39. Stagg-Williams, S. M.; Noronha, F. B.; Fendley, G. and Resasco, D. E. CO_2 Reforming of CH_4 over Pt/ ZrO_2 Catalysts Promoted with La and Ce Oxides. J. Catal. 194 (2000) : 240-249.
40. Choi J-S.; Moon K-I.; Kim Y.G.; Lee J.S.; Kim C-H. and Trimm D.L. Stable carbon dioxide reforming of methane over modified Ni/ Al_2O_3 catalysts. Catalysis Letters. 52 (1998) : 43-47.
41. Santori1, G.F.; Casella1, M.L.; Siri, G.J.; Adúriz, H,R. and Ferrettia1, O.A. Effect of particle size in the hydrogenation of crotonaldehyde on supported Pt and Pt-Sn catalysts. Reaction Kinetics and Catalysis Letters. 75 (2002) : 225-230.



APPENDICES

สถาบันวิทยบริการ
จุฬาลงกรณ์มหาวิทยาลัย

APPENDIX A

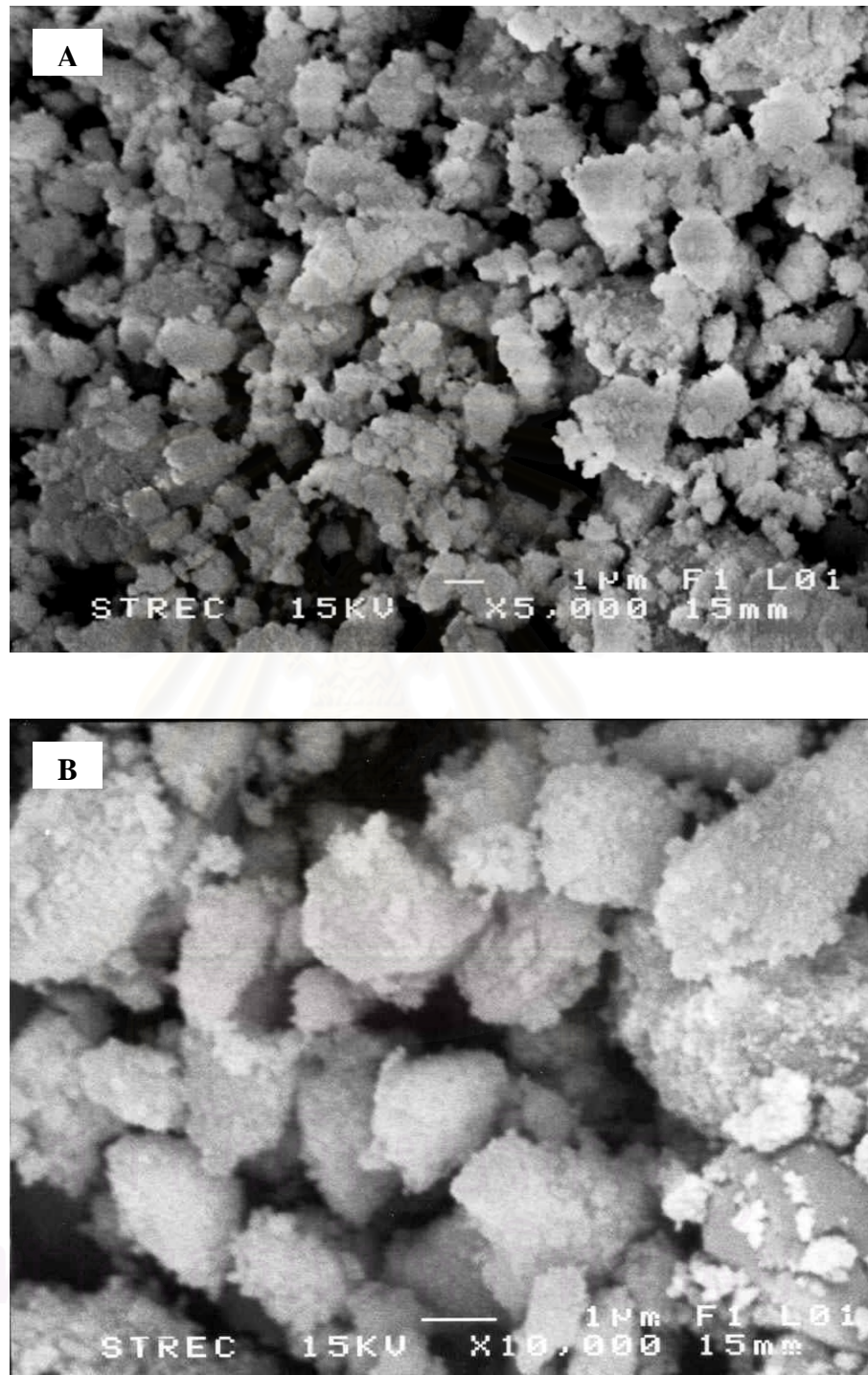


Figure 1 The SEM micrographs of mixed metal oxides of Ni/Mg/Zr prepared by CP method.

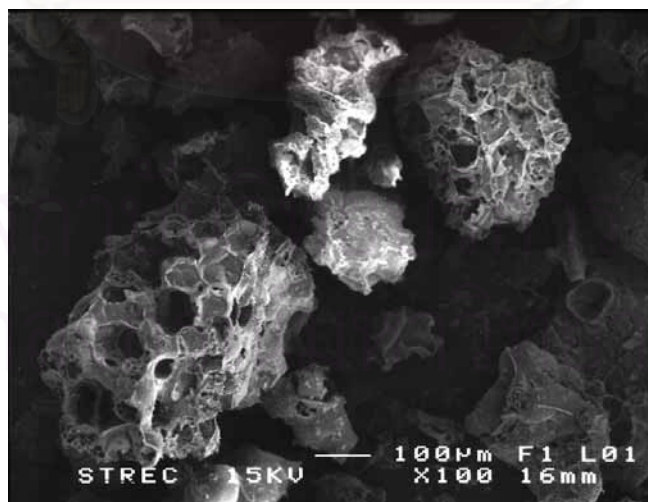
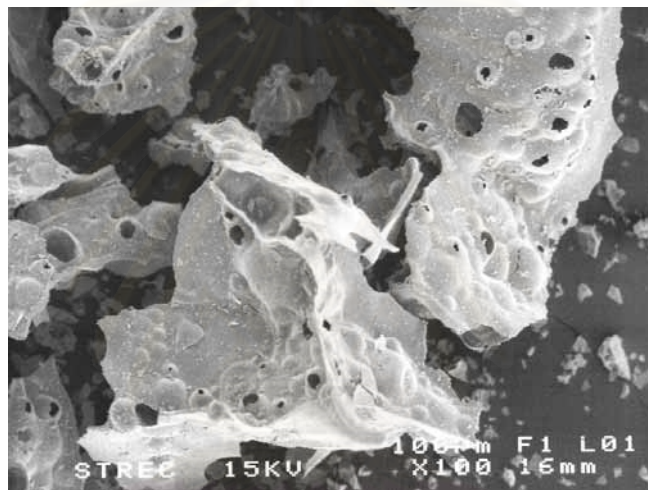
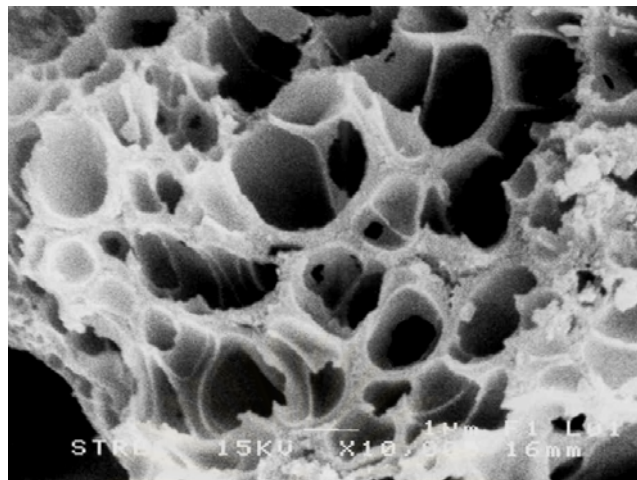


Figure 2 The SEM micrographs of mixed metal oxides of Ni/Mg/Zr prepared by CT method.

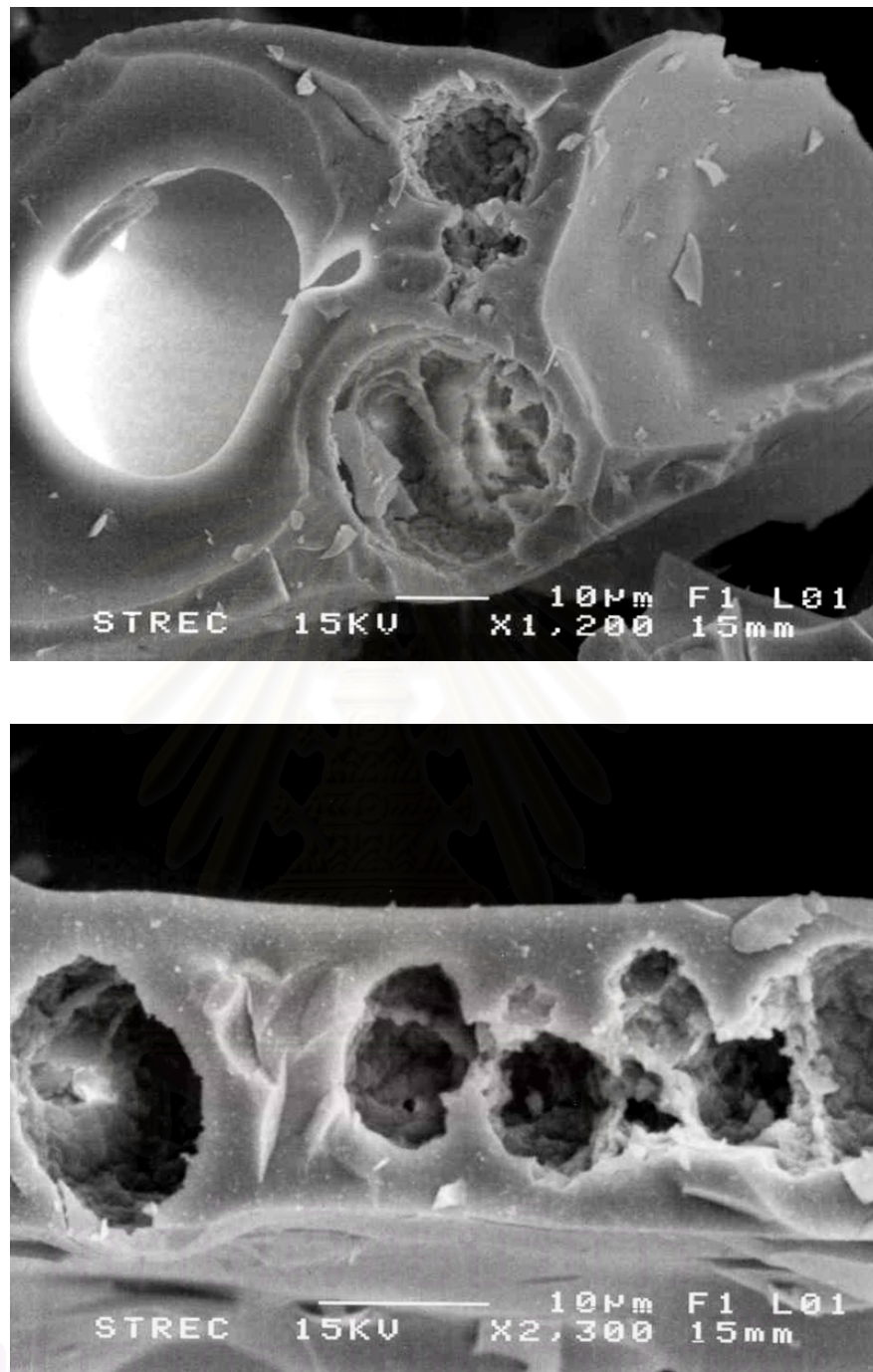


Figure 3 The SEM micrographs of mixed metal oxides of Ni/Mg/Zr prepared by MCT method.

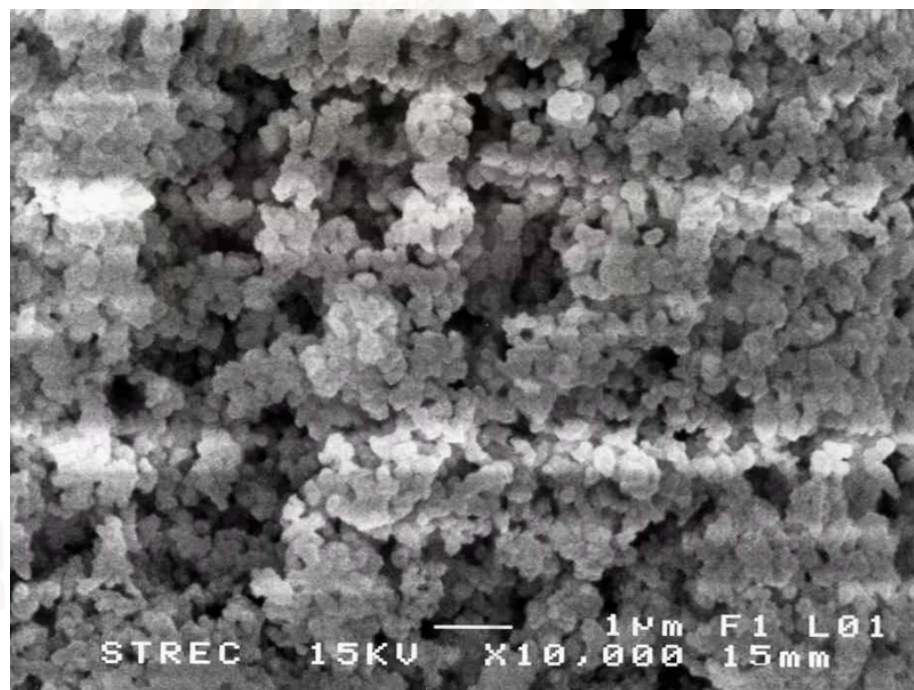
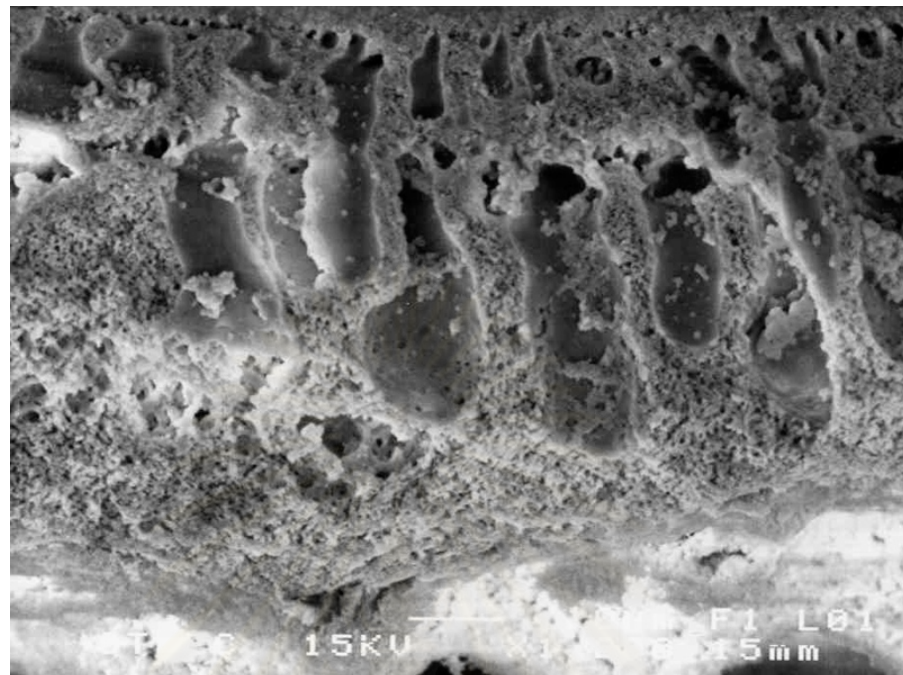


Figure 4 The SEM micrographs of mixed metal oxides of Ni/Mg/Zr prepared by MCTE method.

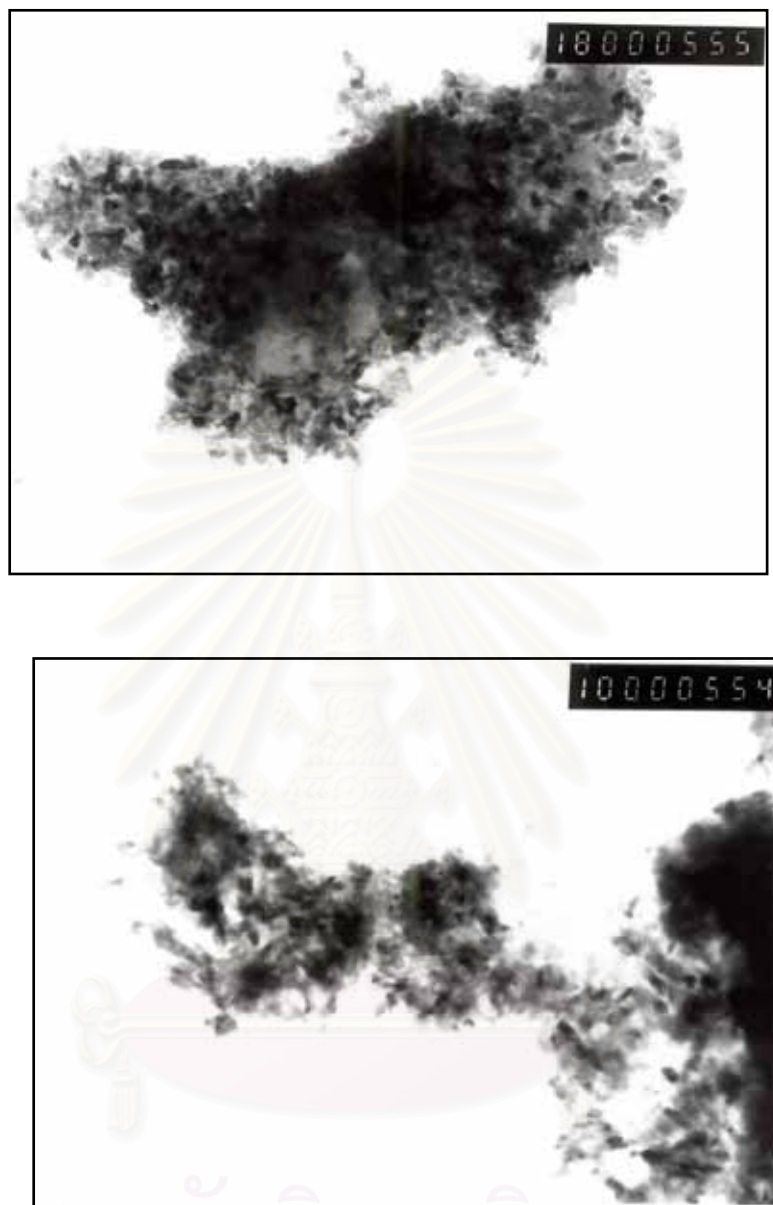


Figure 5 The TEM micrographs of the mixed metal oxides prepared by CP method.

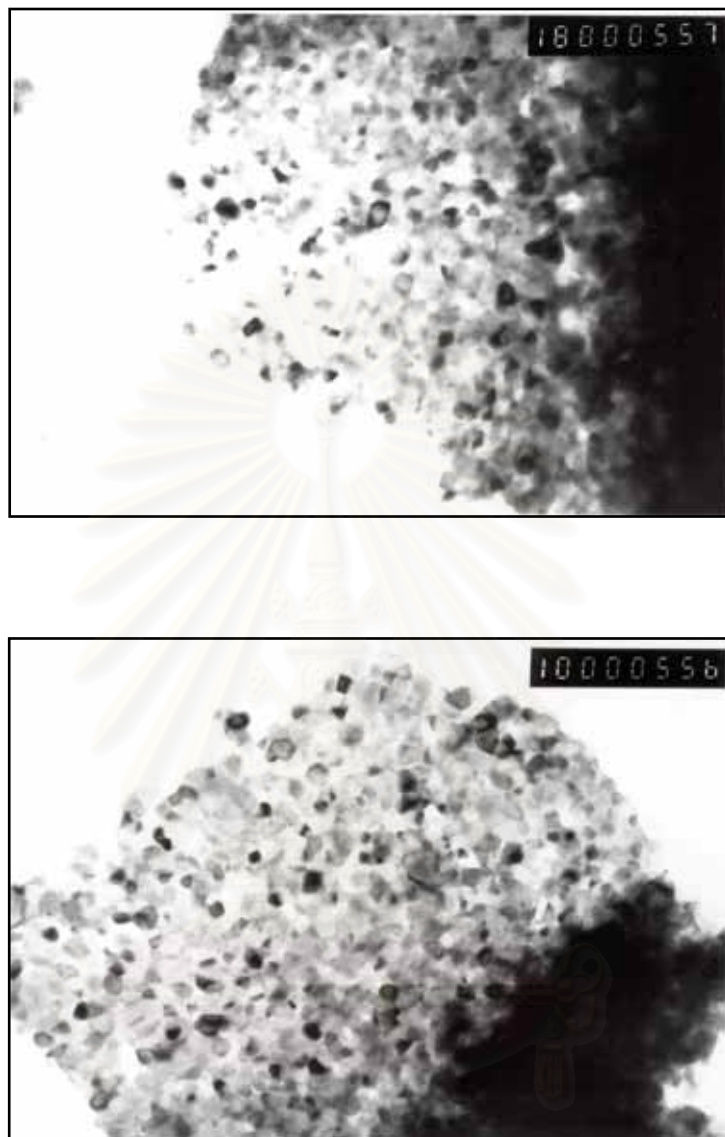


Figure 6 The TEM micrographs of the mixed metal oxides prepared by CT method.

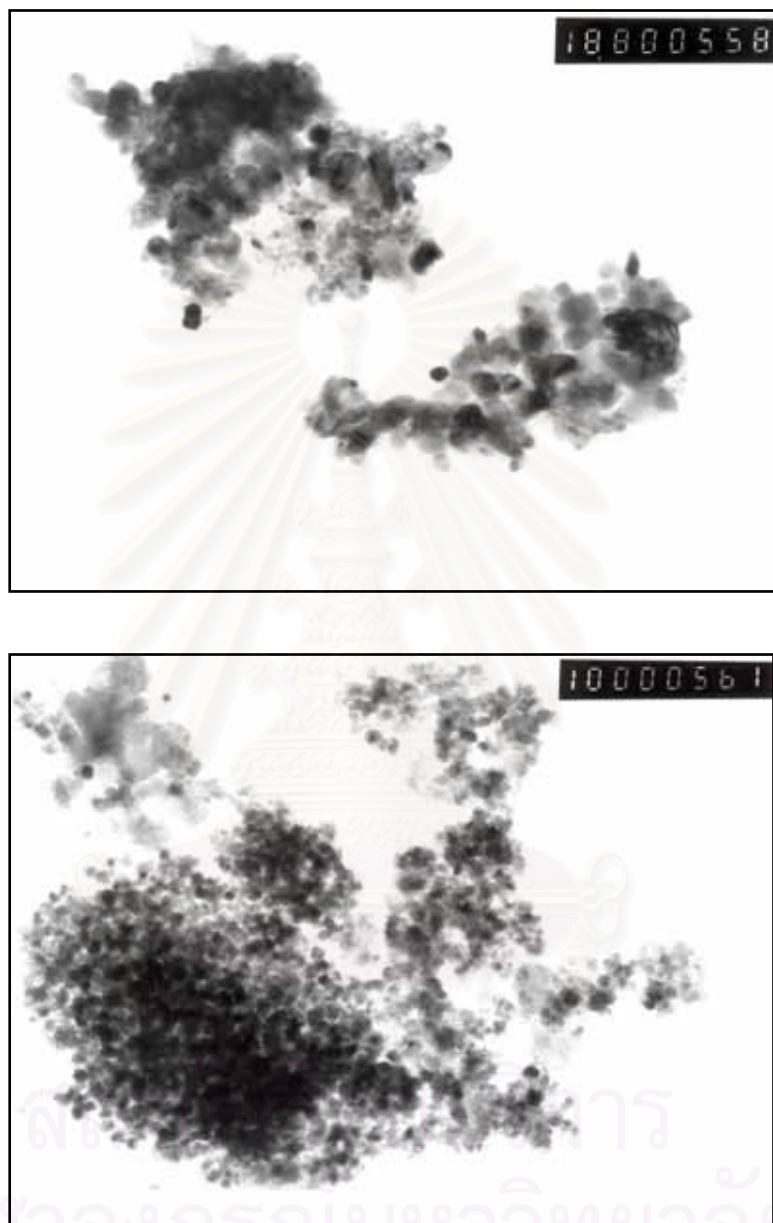


Figure 7 The TEM micrographs of the mixed metal oxides prepared by MCT method.

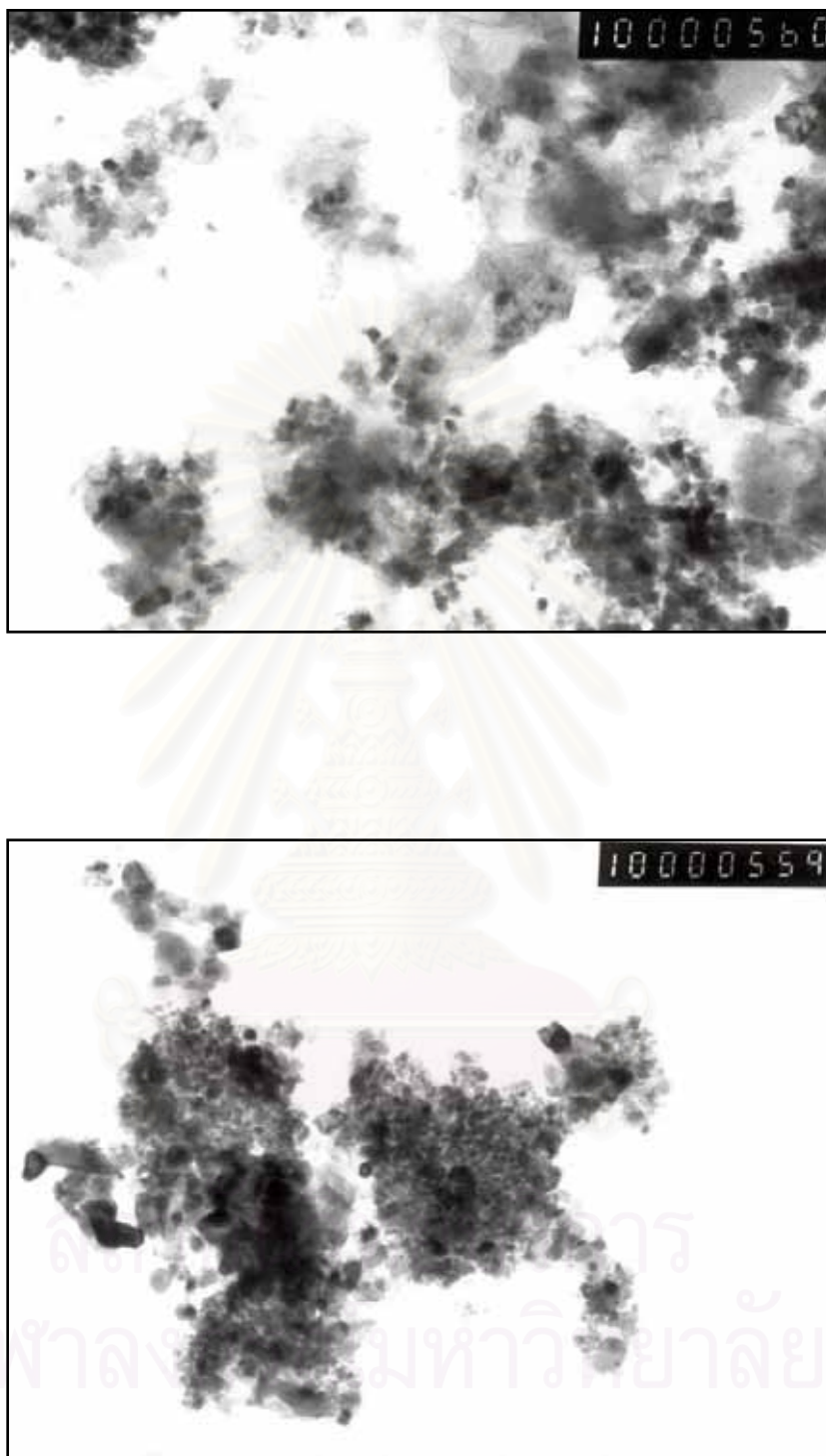


Figure 8 The TEM micrographs of the mixed metal oxides prepared by MCTE method.

APPENDIX B

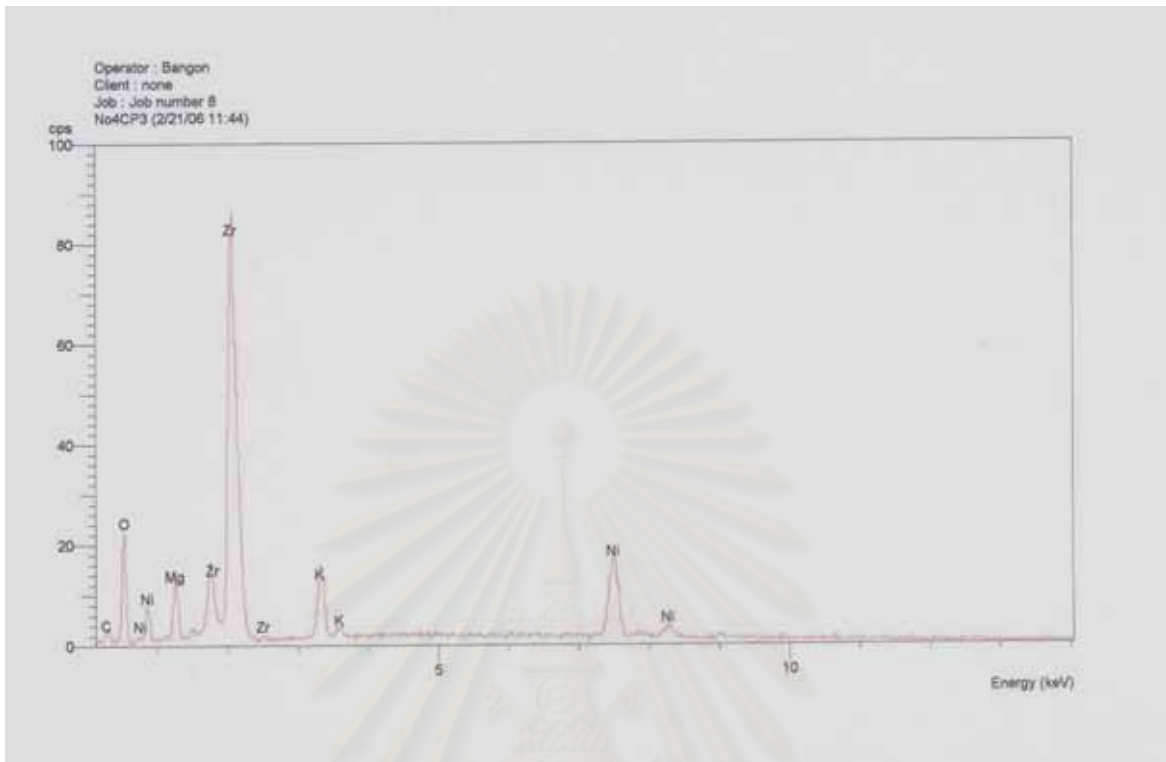


Figure 9 EDX diagrams mixed metal oxides of Ni/Mg/Zr prepared by CP method.

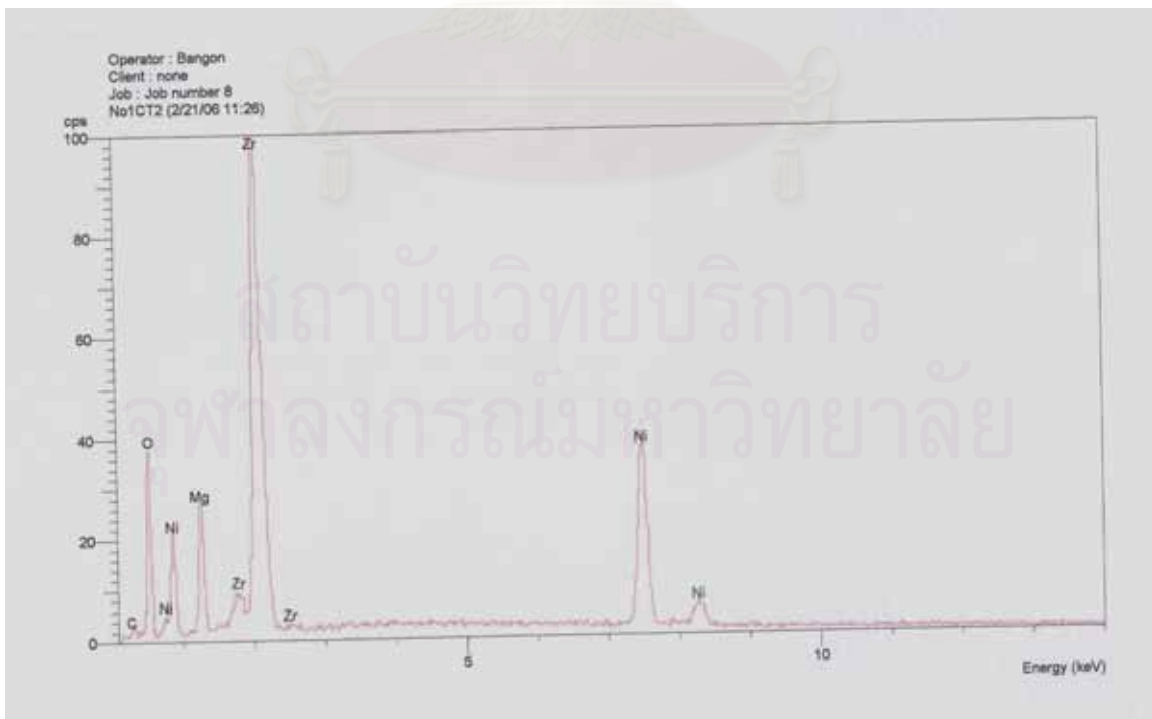


Figure 10 EDX diagrams mixed metal oxides of Ni/Mg/Zr prepared by CT method.

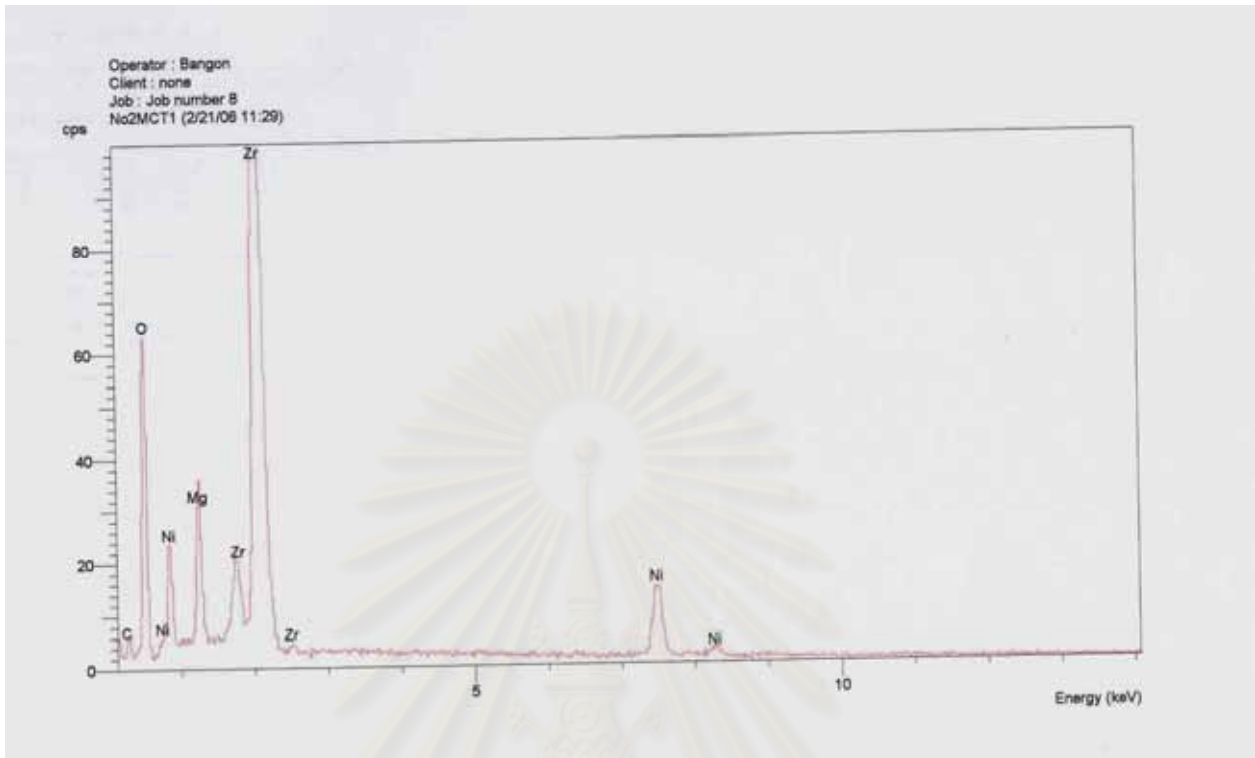


Figure 11 EDX diagrams mixed metal oxides of Ni/Mg/Zr prepared by MCT method.

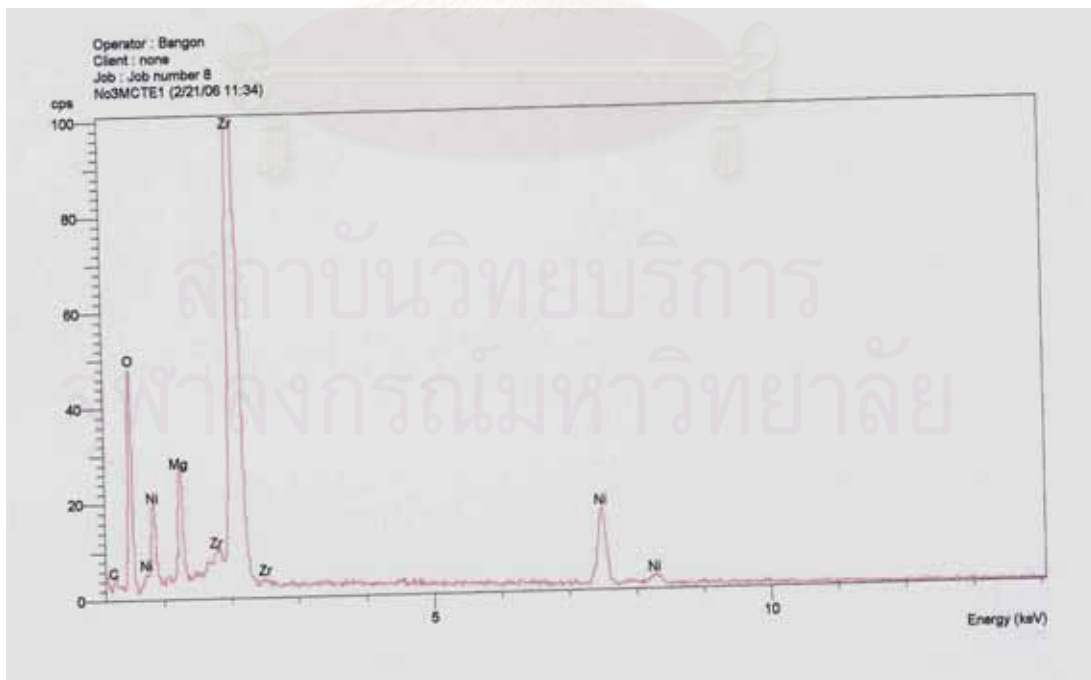


Figure 13 EDX diagrams mixed metal oxides of Ni/Mg/Zr prepared by MCTE method.

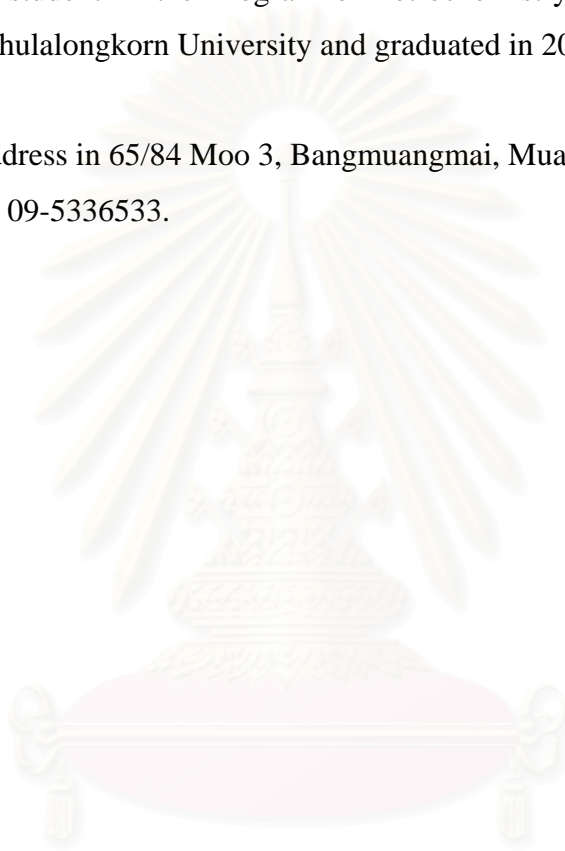


สถาบันวิทยบริการ
จุฬาลงกรณ์มหาวิทยาลัย

VITAE

Mr. Chansak Sukkaew was born on May 5, 1976 in Bangkok. He received B. Sc. Degree in Chemical Engineering from Chulalongkorn University in 1999. Since then, he has been a graduate student in the Program of Petrochemistry and Polymer Science, Faculty of Science, Chulalongkorn University and graduated in 2006.

His present address in 65/84 Moo 3, Bangmuangmai, Muang, Samutprakan, 10270, Thailand. Tel. 09-5336533.



สถาบันวิทยบริการ
จุฬาลงกรณ์มหาวิทยาลัย